

000 SMALL DRAFTS, BIG VERDICT: INFORMATION- 001 002 INTENSIVE VISUAL REASONING VIA SPECULATION 003 004

005 **Anonymous authors**

006 Paper under double-blind review

007 008 ABSTRACT 009

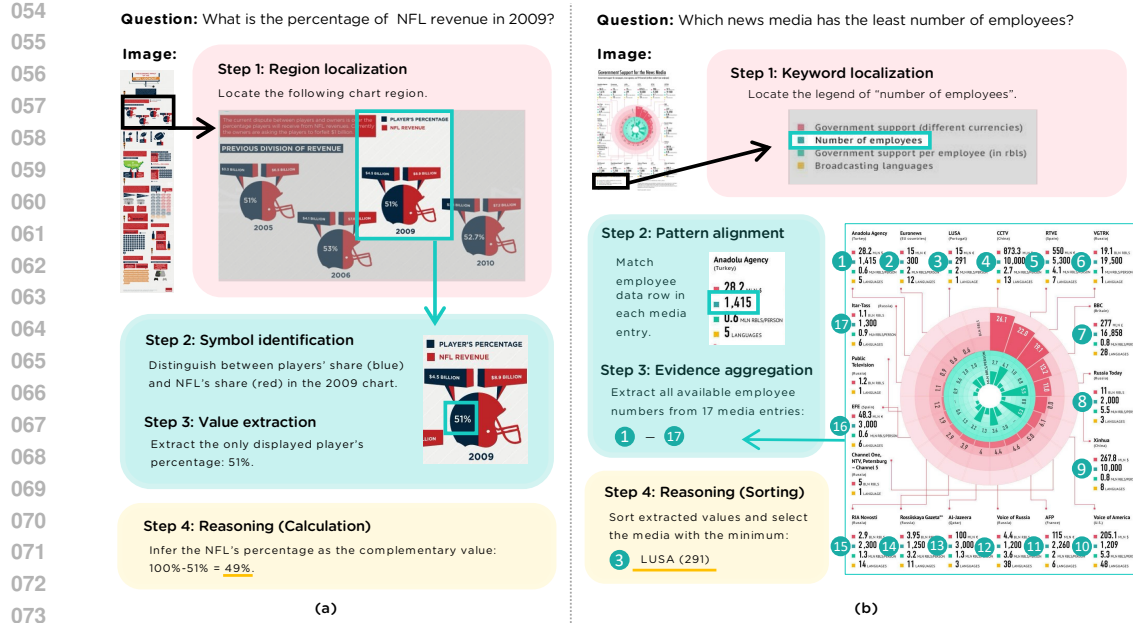
011 Large Vision-Language Models (VLMs) have achieved remarkable progress in
012 multimodal understanding, yet they struggle [when reasoning over](#) information-
013 intensive images that densely interleave textual annotations with fine-grained
014 graphical elements. The main challenges lie in precisely localizing critical cues
015 in dense layouts and multi-hop reasoning to integrate dispersed evidence. We
016 propose Speculative Verdict (SV), a training-free framework inspired by specula-
017 tive decoding that combines multiple lightweight draft experts with a large verdict
018 model. In the draft stage, small VLMs act as draft experts to generate reasoning
019 paths that provide diverse localization candidates; in the verdict stage, a strong
020 VLM synthesizes these paths to produce the final answer, minimizing computa-
021 tional cost while recovering correct answers. To further improve efficiency and
022 accuracy, SV introduces a consensus expert selection mechanism that forwards
023 only high-agreement reasoning paths to the verdict. Empirically, SV achieves
024 consistent gains on challenging information-intensive and high-resolution vi-
025 sual question answering benchmarks, including InfographicVQA, ChartMuseum,
026 ChartQAPro, and HR-Bench 4K. By synthesizing correct insights from multiple
027 partially accurate reasoning paths, SV achieves both error correction and cost-
028 efficiency compared to large proprietary models or training pipelines.

029 1 INTRODUCTION 030

031 Recent advances in large vision-language models (VLMs) have delivered impressive performance
032 on tasks such as image captioning and general visual question answering (VQA) (Li et al., 2025c;
033 Fu et al., 2024). However, these models encounter challenges in information-intensive images that
034 densely interleave diverse textual annotations (legends, labels, captions) with fine-grained graphical
035 elements (charts, diagrams, plots) across multiple scales and formats (Su et al., 2025b). Address-
036 ing this task requires two interdependent capabilities (Figure 1; Ke et al., 2025): (i) comprehensive
037 and precise localization, which involves not only pinpointing the exact positions of critical cues
038 in densely populated layouts but also ensuring that all query-relevant regions are identified; (ii)
039 multi-hop reasoning, which chains visual analysis—encompassing colors, shapes, and spatial rela-
040 tionships—with textual evidence, thereby integrating dispersed cues into a coherent and complete
041 answer. As each reasoning step builds on the accuracy of the previous one, any intermediate er-
042 ror can propagate through the entire chain, making the overall process highly error-sensitive and
043 difficult to correct retrospectively.

044 Existing work tackles information-intensive visual reasoning with search-based zoom-in pipelines
045 that enlarge local regions for detailed reasoning. Specifically, learning-based methods train rein-
046 force learning policies to guide zoom operations iteratively (Zheng et al., 2025; Su et al., 2025a;
047 Fan et al., 2025; Zhang et al., 2025b). Enhancing its performance would demand costly fine-grained
048 supervision. Moreover, training-free methods perform cropping based on internal attention or con-
049 fidence scores (Zhang et al., 2025a; Shen et al., 2024; Wang et al., 2025c). Yet in dense layouts, we
050 find these signals correlate weakly with true relevance, misleading the model into visually similar but
051 irrelevant areas. Consequently, these tool-driven designs fail to capture all evidence for multi-hop
052 reasoning, leaving the core challenges of information-intensive visual reasoning unsolved.

053 To overcome these limitations, we propose Speculative Verdict (SV), a training-free framework
inspired by speculative decoding that combines small draft visual experts with a large verdict



068 Figure 1: Examples of correct reasoning paths for information-intensive VQA tasks. They illustrate
069 distinct paths: (a) focuses on the localization of a specific chart, symbol identification, and reasoning
070 from a single percentage value; (b) focuses on keyword-based localization, evidence aggregation
071 from multiple entries across the entire image, and cross-entity sorting to select the minimum.

072 model (Leviathan et al., 2023). The framework operates in two stages (Figure 2): (1) Draft stage:
073 multiple lightweight VLMs serve as draft experts, each generating a reasoning path that offers di-
074 verse localization candidates; (2) Verdict stage: a large VLM acts as a strong verdict, which receives
075 the reasoning paths as contextual evidence, distinguishes the correct information, and outputs the
076 final answer. SV directly tackles core challenges through complementary strengths: draft experts
077 expand evidence coverage across scattered regions, while the verdict prevents error propagation by
078 synthesizing these multiple perspectives. Importantly, unlike using a large proprietary model to
079 reason over every image section, SV invokes the verdict only once to yield a concise final answer.
080 To further balance accuracy and efficiency, SV introduces a consensus expert selection mechanism in the
081 draft stage, ensuring that only reasoning paths with strong agreement are forwarded to the verdict.

082 We evaluate **SV** on information-intensive VQA benchmarks, including InfographicVQA (Mathew
083 et al., 2021), ChartMuseum (Tang et al., 2025), and ChartQAPro (Masry et al., 2025), which demand
084 reasoning over dense textual and visual content. As a training-free framework, SV consistently out-
085 performs strong open-source models, large proprietary models, and perception-focused search meth-
086 ods while remaining cost-efficient. In particular, SV yields average gains of 4% over small VLMs
087 as draft experts and 10% over GPT-4o (Hurst et al., 2024) as verdict. Beyond overall gains, SV suc-
088 cessfully corrects 47-53% of cases where majority voting or the verdict model alone fails, thereby
089 reducing vulnerability to error propagation in information-intensive visual reasoning. Furthermore,
090 SV surpasses all baselines on HR-Bench 4K (Wang et al., 2025b), a benchmark for high-resolution
091 visual perception, underscoring its effectiveness in challenging multimodal reasoning scenarios.

100 2 RELATED WORK

101 **Vision-Language Model Reasoning with Tools.** Recent research has explored enhancing VLM
102 perception by manipulating input images with zooming operations to locate relevant regions. (1) Promp-
103 ting-based methods exploit internal signals of VLMs to decide where to zoom. ViCrop (Zhang
104 et al., 2025a) leverages models' attention maps to highlight query-related regions, thereby gener-
105 ating automatic visual crops. Other works perform tree-based search, where models evaluate candidate
106 sub-images with confidence scores to iteratively narrow down to relevant regions (Shen et al., 2024;
107 Wang et al., 2025c). However, such signals align poorly with the required evidence in information-

108 intensive images, since queries often require reasoning across multiple dispersed regions. (2) Rein-
 109 force learning approaches instead optimize policies that interleave visual zooming with textual
 110 reasoning (Zheng et al., 2025; Su et al., 2025a; Fan et al., 2025; Zhang et al., 2025b). By calling
 111 zooming tools within the agentic framework, these methods adaptively crop regions and concatenate
 112 them into the reasoning trajectory, enabling more active evidence gathering. Yet these methods still
 113 fall short on information-intensive images, requiring costly task-specific training to scale.

114 **General Vision-Language Model Reasoning.** Recent work has also explored other paradigms that
 115 enhance VLM reasoning. Prompt-enhanced VLMs use chain-of-thought prompting to articulate in-
 116 termediate observations and sub-goals, yielding more structured reasoning (Xu et al., 2025; Mitra
 117 et al., 2024; Shao et al., 2024). RL-enhanced methods further optimize these trajectories via super-
 118 viewed fine-tuning and reinforcement learning, inspired by reasoning-oriented models such as GPT-o1
 119 and DeepSeek-R1 (Huang et al., 2025; Ma et al., 2025; Jaech et al., 2024; Guo et al., 2025). Recently,
 120 agentic frameworks treat the VLM as a planner that decomposes queries and actively chooses ac-
 121 tions, either invoking explicit visual tools or performing implicit latent-space reasoning (Wu & Xie,
 122 2024; Hu et al., 2024; Qi et al., 2024; Yang et al., 2025b; Wu et al., 2025). However, they remain
 123 vulnerable to imprecise or weakly supervised visual operations and error propagation.

124 **LMM-as-a-Judge.** Large multimodal models (LMMs) increasingly serve as general-purpose eval-
 125 uators for vision-language tasks (Zhang et al., 2023; Ge et al., 2025; Li et al., 2025b). Specifically,
 126 LMM judges are prompted or trained to score candidates, produce rankings, or select the best answer
 127 given the task context, and instruction (Xiong et al., 2025). These judges can deliver fine-grained
 128 evaluations for open-ended generation and reasoning tasks, and are increasingly used as scalable
 129 supervision signals for stages such as alignment, retrieval, and reasoning (Li et al., 2025a). In our
 130 framework, the verdict model acts as an off-the-shelf multimodal judge that filters informative cues
 131 from diverse drafts and synthesizes an answer on information-intensive images.

132 **Speculative Decoding.** Speculative decoding is a draft-then-verify decoding paradigm to accelerate
 133 LLM inference (Xia et al., 2024). Specifically, it uses a draft model to generate future tokens, and
 134 a larger target model verifies them via parallel rejection sampling. Recent work extends acceptance
 135 from token-level equivalence to step-level semantic similarity to speed up reasoning (Yang et al.,
 136 2025a; Pan et al., 2025; Fu et al., 2025b; Liao et al., 2025). Collaborative decoding via Specula-
 137 tion (Fu et al., 2025a) further applies speculative decoding with multiple draft LLMs by verifying
 138 proposals against a combined distribution of drafts and target, yielding greater speedups. However,
 139 they mainly target speed in LLM inference and do not address [visual reasoning challenges](#).

140 3 SPECULATIVE VERDICT

142 Speculative decoding is an inference-time optimization originally developed to mitigate the latency
 143 of autoregressive generation (Leviathan et al., 2023). The approach employs a draft-then-verify
 144 paradigm: (i) a small, fast draft model proposes one or more future tokens speculatively, and (ii) a
 145 large, accurate base model verifies these proposals in parallel, accepts or revises the proposals, and
 146 generates output that is consistent with the base model’s distribution (Xia et al., 2024; Zhang et al.,
 147 2024). This token-level process speeds up inference by committing several tokens at once, while
 148 maintaining quality by discarding continuations that diverge from the base model’s distribution.

149 The key insight is that draft models expand coverage quickly, while the verifier ensures correctness.
 150 Although this idea has been mainly applied to accelerate text generation, its high-level principle is
 151 also well-suited for information-intensive multimodal reasoning.

153 3.1 METHOD OVERVIEW

155 Information-intensive visual question answering (VQA) requires models to localize query-relevant
 156 regions, perceive diverse fine-grained textual and visual details, and integrate dispersed evidence
 157 into a single correct answer. These tasks are highly error-sensitive as elaborated in Section 1: a
 158 single misread or mislocalized element often leads to a completely wrong prediction.

159 To address this challenge, we adapt the draft-then-verify paradigm of speculative decoding to mul-
 160 timodal reasoning. Unlike its original use for inference acceleration, we repurpose the paradigm to
 161 improve robustness and error correction in information-intensive visual reasoning. On a high level,
 our Speculative Verdict (SV) framework operates in two stages (Figure 2):

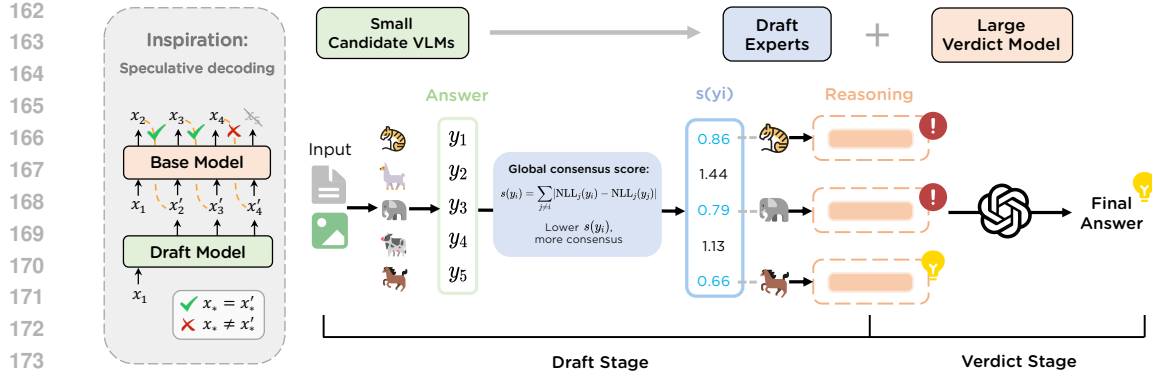


Figure 2: Overview of Speculative Verdict (SV). Inspired by speculative decoding, SV operates in two stages. In the draft stage, given an input question-image pair, k small candidate VLMs first generate candidate answers, from which we compute a global consensus score $s(y_i)$ for each answer based on pairwise NLL differences. We then select m draft experts with the strongest consensus to generate reasoning paths. In the verdict stage, the large verdict model verifies and integrates these paths to yield the final answer.

- (i) **Draft stage**, where multiple lightweight VLMs are selected as draft experts to provide diverse reasoning paths (Section 3.2);
- (ii) **Verdict stage**, where a large VLM acts as verdict to verify, refine, and synthesize these reasoning paths into the final prediction (Section 3.3).

3.2 DRAFT STAGE

Chain-of-Thought (CoT) prompting exposes models’ intermediate reasoning steps in an explicit, stepwise form (Wei et al., 2022). This is critical for information-intensive VQA, where solving a question requires a sequence of localization, evidence extraction, and analytic operations (Figure 1). However, current VLMs often lack fine-grained perception and localization on densely annotated images, and existing tool-driven zoom-in methods are ineffective as elaborated in Section 2. We therefore utilize multiple VLMs to produce reasoning paths rather than a single direct answer, so that the subsequent verdict can verify and synthesize structured evidence. Concretely, given an image-question pair (x, q) , we select m lightweight VLMs $\{M_1, \dots, M_m\}$ as draft experts from a pool of k candidate VLMs via a consensus-based selection mechanism (detailed in Section 3.4). Each selected expert M_i is then prompted with a CoT template to output a reasoning path r_i .

We observe that each reasoning path r_i provided by draft experts typically includes: (i) global scan and localization proposals that identify query-related regions, sections, or subplots, often referencing axes, titles, or captions; (ii) evidence extraction, which transforms visual or textual elements into structured cues, including reading legends, mapping colors to series, parsing axis labels, or assembling lists of values or tokens for subsequent operations; (iii) analytic and reasoning operations, which operate over the extracted cues to derive higher-level conclusions, such as filtering or selecting relevant entities, computing differences, sorting across panels, and cross-referencing dispersed cues. As shown in the running case (Figure 3), different experts may match legends to charts differently; some correctly gather the required cues while others misread adjacent values. This diversity yields a complementary but potentially noisy pool of reasoning signals.

3.3 VERDICT STAGE

The set $\{r_i\}$ captures diverse cues, offering richer evidence but also introducing contradictions, which motivates the need for a verdict stage to verify and integrate them. Answer-level ensembling (e.g., majority voting) often fails in minority-correct scenarios where many experts converge on the same incorrect decision, such as mislocalizing the query-related region or misreading fine-grained textual details, even after correct localization. This failure mode is frequently observed in information-intensive reasoning (as illustrated in Figure 3). Rather than discarding minority opin-

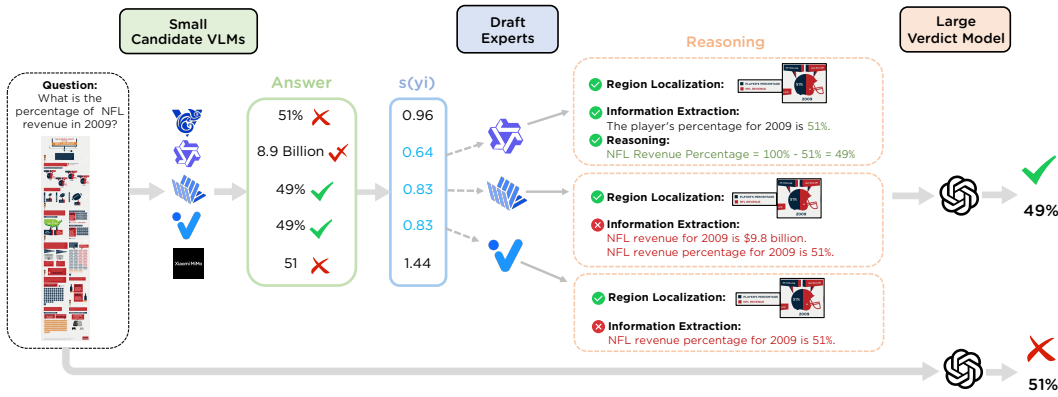


Figure 3: An illustration of Speculative Verdict on InfographicVQA. Five candidate VLMs first produce candidate answers, with only two providing the correct result. Consensus scoring ranks answers by agreement, and the three with the lowest scores are selected as draft experts. Although some experts commit extraction errors (confusing player’s share with NFL revenue), the verdict synthesizes their reasoning paths and successfully recovers the correct answer (49%). This illustrates SV’s ability to identify reliable experts and achieve error correction.

ions through majority voting, we leverage a stronger model as a verdict to validate grounding, resolve conflicts, and synthesize coherent reasoning from the draft paths.

Specifically, given the image-question pair (x, q) and the drafts’ reasoning paths $\{r_i\}_{i=1}^m$, we prompt the verdict model J with: (i) the original image x as visual input, and (ii) a textual prompt containing the question q and the concatenated reasoning paths $\{r_i\}_{i=1}^m$ as context. The verdict processes this multimodal input in a single inference call and outputs the final answer:

$$y = J(x, q, \{r_i\}_{i=1}^m).$$

In this design, the verdict acts not as a voter but as a synthesizer. It evaluates grounding consistency, identifies contradictions across reasoning paths, and integrates consistent cues into a coherent prediction. The case in Figure 3 illustrates this intended role: when only one draft extracts the correct evidence, the verdict is designed to recover it by contrasting against competing but inconsistent paths.

This setup enables us to leverage the reasoning capabilities of large models while keeping the inference cost manageable. The verdict stage reduces the expensive autoregressive decoding phase by concentrating computation in prefill: it processes thousands of tokens from multiple draft reasoning paths as prefill input and produces only several answer tokens sequentially. This design avoids invoking large models iteratively for analyzing each image section separately or generating lengthy rationales, both of which would substantially increase decoding costs.

3.4 CONSENSUS EXPERT SELECTION

To keep the verdict input both efficient and accurate, we introduce a training-free expert selection mechanism at the beginning of the draft stage (Section 3.2). Since each question in information-intensive VQA has a unique correct answer, consensus among model answers naturally indicates which reasoning paths are more reliable. Therefore, the key idea here is to measure agreement among candidate answers and retain only those with stronger peer consensus. This mechanism is computed efficiently by prefilling the question and answer tokens, with each draft decoded only once, making it plug-and-play with minimal overhead.

Consensus Score. We define a consensus score that measures how strongly a candidate VLM’s answer is agreed by its peers. Formally, let x be the input image and $q = (q_1, \dots, q_n)$ the question tokens. From the pool of k candidate VLMs $\{M_i\}_{i=1}^k$, each model produces a candidate answer $y_i = (y_{i,1}, \dots, y_{i,T})$. For a peer model M_j ($j \neq i$) in the pool, we measure how plausible it finds y_i by computing the negative log-likelihood (NLL) of the concatenated input (x, q, y_i) , i.e., the original

270 image together with the question tokens followed by the candidate answer tokens:
 271

$$272 \quad \text{NLL}_j(y_i) = -\frac{1}{T} \sum_{t=1}^T \log p_{M_j}(y_{i,t} \mid x, q_{\leq n}, y_{i,<t}).$$

$$273$$

$$274$$

275 To account for calibration differences, we normalize against M_j 's own answer y_j , thus *relative*
 276 *consensus score* from M_j 's perspective is:
 277

$$278 \quad s_j(y_i) = |\text{NLL}_j(y_i) - \text{NLL}_j(y_j)|, \quad j \neq i,$$

$$279$$

$$280$$

281 where a smaller $s_j(y_i)$ indicates stronger agreement, as M_j finds y_i nearly as plausible as its own
 282 answer y_j .
 283

284 To capture overall agreement rather than pairwise consistency, we define the *global consensus score*
 285 of candidate y_i by summing across all peers:
 286

$$287 \quad s(y_i) = \sum_{j \neq i} s_j(y_i),$$

$$288$$

289 which quantifies the overall level of peer consensus for M_i 's answer, and a lower $s(y_i)$ indicates
 290 stronger agreement and thus higher reliability.
 291

292 **Consensus Expert Selection Strategy.** We adopt a cross-all strategy that selects the *m* VLMs with
 293 the strongest consensus, measured by the lowest consensus scores, from the pool of *k* candidates.
 294 As described in Section 3.2, the *m* selected VLMs become the draft experts to generate detailed reasoning
 295 paths forwarded to the verdict (Figure 3 illustrates this process). By aggregating agreement
 296 across all peers, this strategy provides a holistic measure of reliability. It thus yields a subset of reasoning
 297 paths that are well-grounded and compact in size, balancing informativeness and efficiency.
 298

299 4 EXPERIMENTS

$$300$$

301 4.1 SETUPS

$$302$$

303 **Configuration Details.** We set the draft pool size to $k = 5$ considering efficiency and select $m = 3$
 304 draft experts in our main experiments. Ablation studies over different m values are reported in
 305 Section 4.5. The draft pool consists of the following VLMs for expert selection: Qwen2.5-VL-
 306 7B-Instruct (Bai et al., 2025), MiMo-VL-7B-RL (Xiaomi, 2025), InternVL3-8B (Zhu et al., 2025),
 307 GLM-4.1V-9B-Thinking (Team et al., 2025b), Ovis2.5-9B (Lu et al., 2025). These models are
 308 chosen as candidate VLMs based on their strong performance on multimodal benchmarks and their
 309 diverse architectural designs. For the verdict models, we employ GPT-4o (Hurst et al., 2024) and
 310 Qwen2.5-VL-72B-Instruct respectively, given their superior ability in visual reasoning. In particular,
 311 for information-intensive image benchmarks, we preprocess images with PP-StructureV3 (Cui
 312 et al., 2025) to produce a layout-preserving structured format, provided together with the original
 313 image as auxiliary input to the verdict model.

314 **Baselines.** We compare SV with proprietary models GPT-4o and GPT-4o-mini, and the large open-
 315 source model Qwen2.5-VL-72B-Instruct as it is one of our verdicts. We also evaluate SV against
 316 draft experts mentioned above. These baselines are evaluated under the same chain-of-thought
 317 prompting template in Appendix M. Additionally, we include DeepEyes (Zheng et al., 2025) and
 318 Pixel-Reasoner (Su et al., 2025a) as representative tool-driven baselines with zoom-in operations.
 319

320 **Benchmarks.** We evaluate SV on three information-intensive benchmarks and extend the evalua-
 321 tion to a representative high-resolution benchmark, providing a comprehensive assessment of fine-
 322 grained visual reasoning: InfographicVQA (Mathew et al., 2021), ChartMuseum (Tang et al., 2025),
 323 ChartQAPro (Masry et al., 2025) and HR-Bench 4K (Wang et al., 2025b). InfographicVQA collects
 324 infographics with an average high resolution over 2k, designed to test reasoning over layout, graph-
 325 ical and textual content, including operations such as counting, sorting, and basic arithmetic. Chart-
 326 Museum and ChartQAPro introduce substantially greater visual reasoning complexity by covering
 327 a broad spectrum of real-world chart types and question formats, revealing a large performance gap
 328 between current Large VLMs and humans. These benchmarks require models to visually ground
 329 relevant regions, extract information, and conduct reasoning to answer queries.
 330

324
 325 Table 1: Results on test sets of four benchmarks. InfographicVQA, ChartMuseum, and ChartQAPro
 326 are information-intensive VQA benchmarks, while HR-Bench 4K focuses on high-resolution per-
 327 ception. We compare SV against closed-source, open-source VLMs, and **tool-driven methods**. \dagger
 328 denotes results reported in the original papers and all other results are reproduced by ourselves. The
 329 best results for each benchmark are highlighted in **bold** and the second-best results are underlined.

Model	Param Size	InfographicVQA ANLS	ChartMuseum Acc	ChartQAPro Acc	HR-Bench 4K Acc
<i>Closed-source VLMs</i>					
GPT-4o	—	76.5	42.7	52.6	67.4
GPT-4o-mini	—	67.2	31.5	44.1	53.8
<i>Open-source VLMs</i>					
Qwen2.5-VL-Instruct	7B	79.8	29.5	51.0	73.0
MiMO-VL-RL (think)	7B	83.5	29.0	57.3	72.3
InternVL3	8B	72.3	25.9	45.1	68.0
GLM-4.1V-Thinking	9B	84.8	48.0	56.2	72.3
Ovis2.5	9B	81.7	34.0	55.9	69.5
Qwen2.5-VL-Instruct	72B	84.2	40.7	60.7	<u>73.1</u>
<i>Tool-driven method</i>					
DeepEyes	7B	75.5	28.0	48.7	73.0
Pixel-Reasoner	7B	<u>84.0</u> \dagger	<u>25.9</u>	<u>39.3</u>	—
SV w/ GPT-4o Verdict	—	88.4	49.3	64.0	71.4
Δ (vs. GPT-4o)	—	<u>+11.9</u>	<u>+6.6</u>	<u>+11.4</u>	<u>+4.0</u>
SV w/ Qwen2.5-VL-72B-Instruct Verdict	—	<u>86.7</u>	<u>48.2</u>	<u>63.0</u>	75.6
Δ (vs. Qwen2.5-VL-72B-Instruct)	—	<u>+2.5</u>	<u>+7.5</u>	<u>+2.3</u>	<u>+2.5</u>

346 Table 2: Results on additional multimodal reasoning benchmarks. We evaluate on MathVista-
 347 testmini and 1000 randomly sampled complex questions from TallyQA to assess generalization.

Model	Param Size	TallyQA-Complex Acc	MathVista Acc
<i>Closed-source VLMs</i>			
GPT-4o	—	<u>75.4</u>	65.1
<i>Open-source VLMs</i>			
Qwen2.5-VL-Instruct	7B	72.4	68.2
MiMO-VL-RL	7B	72.0	<u>80.3</u>
InternVL3	8B	70.1	72.7
GLM-4.1V-Thinking	9B	73.9	78.9
Ovis2.5	9B	71.9	77.3
SV w/ GPT-4o Verdict	—	76.9	82.9
Δ (vs. GPT-4o)	—	<u>+1.5</u>	<u>+17.8</u>

350 We further assess generalization to high-resolution [perception](#) on HR-Bench 4K. It comprises two
 351 sub-tasks: FSP (Fine-grained Single-instance Perception) and FCP (Fine-grained Cross-instance
 352 Perception), stressing small-object perception and cross-instance reasoning. [We also test on two ad-](#)
 353 [ditional multimodal reasoning benchmarks, TallyQA \(Acharya et al., 2019\) and MathVista \(Lu et al.,](#)
 354 [2023\), covering open-ended counting with relational reasoning and mathematical visual reasoning.](#)

355 4.2 RESULTS ON INFORMATION-INTENSIVE BENCHMARKS

356 As shown in Table 1, SV demonstrates superior performance across all benchmarks, outperforming
 357 a wide range of baselines. Based on the results, we have the following key observations:

358 (i) **SV shows consistent gains over all strong draft experts’ baselines**, with improvements of 3.6%
 359 on InfographicVQA, 1.3% on ChartMuseum, and 6.7% on ChartQAPro with GPT-4o as verdict. SV
 360 also achieves comparable gains with Qwen2.5-VL-72B-Instruct as a verdict.

361 (ii) **Importantly, SV enables strong error correction beyond simple answer aggregation**.
 362 Figure 4 analyzes SV’s performance on cases where the verdict itself fails, categorized by expert
 363 correctness (minority-correct, majority-correct, zero-correct). Across benchmarks, SV recovers
 364 47-53% of minority-correct cases, where few draft experts are correct and the verdict alone also
 365 fails (case in Figure 3). Moreover, SV even recovers 2.5-4.5% of zero-correct cases, where
 366 neither the drafts nor the verdict answers correctly (case in Appendix L). In these [hard](#) cases, SV
 367 [exploits complementary reasoning strengths across draft experts \(e.g., extraction, localization,](#)

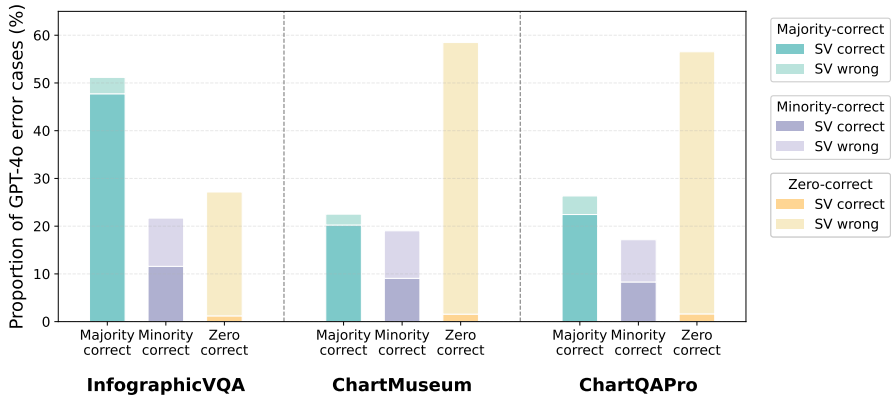


Figure 4: SV’s correction ability on verdict’s error cases across information-intensive benchmarks (GPT-4o as verdict). We consider only cases where the verdict itself fails, to isolate SV’s independent correction capacity. For each benchmark, three bars denote expert correctness categories (majority-correct, minority-correct, and zero-correct), defined by how many selected experts provide the correct answer. Within each category, the bars are split into the proportion corrected by SV (dark) versus not corrected (light). More details can be found in Appendix D.

color matching) (see detailed analysis in Appendix I). This complementarity allows the verdict to synthesize partially correct evidence across reasoning paths while rejecting misleading signals. Thus, SV achieves effective correction where traditional ensemble methods fail.

(iii) **SV strengthens large verdict models significantly**, and using GPT-4o as verdict delivers stronger results due to its reasoning advantage on information-intensive benchmarks. Specifically, when GPT-4o is used as verdict, SV surpasses the GPT-4o baseline by 11.9% on InfographicVQA, 6.6% on ChartMuseum, and 11.4% on ChartQapro. These improvements come with reduced inference cost for the large verdict model, demonstrating that SV can outperform much larger or proprietary LVLMs in a cost-efficient manner.

(iv) **SV substantially outperforms representative tool-driven pipeline DeepEyes and Pixel-Reasoner.** Specifically, it improves over DeepEyes by +12.9% on InfographicVQA, +21.3% on ChartMuseum, and +11.3% on ChartQapro and it also exceeds Pixel-Reasoner by clear margins. While these methods benefit from zoom-in operations, such operations are often under-triggered or misdirected on dense infographics (see Appendix K). Thus, it struggles with global comparison and dispersed evidence synthesis. Yet, SV’s reasoning-path synthesis enables it to integrate evidence across regions reliably without relying on predefined tool-based visual search.

4.3 RESULTS ON HIGH-RESOLUTION BENCHMARK

We further assess generalization to high-resolution images using HR-Bench 4K to evaluate whether SV can enhance fine-grained visual perception. The key observations are as follows (Table 1):

(i) With Qwen2.5-VL-72B-Instruct as verdict, SV achieves its largest margin, surpassing the best-performing draft expert by 2.6% and even outperforming the verdict itself by 2.5%. The superior performance of Qwen2.5-VL-72B as verdict on this task correlates with its stronger visual localization capabilities, indicating verdict selection should align with task-specific requirements.

(ii) SV also exceeds DeepEyes, which is explicitly trained with zoom-in tools for iterative visual search on high-resolution perception. This highlights SV’s ability to generalize to high-resolution tasks, where accurate recognition of small objects is critical. Aligning perceptually strong draft experts with a verdict thus provides a simpler yet effective solution for high-resolution reasoning.

4.4 RESULTS ON MULTIMODAL REASONING BENCHMARKS

To examine SV’s broader generalization, we further evaluate it on two additional multimodal reasoning benchmarks: TallyQA (counting) and MathVista (mathematical reasoning). Table 2 shows that SV provides consistent gains, outperforming the strongest draft expert by 3.0% on TallyQA-

432 Complex and 2.6% on MathVista, and improving over GPT-4o by 1.5% and 17.8%, respectively.
 433 These results demonstrate that SV generalizes to diverse visual reasoning tasks.
 434

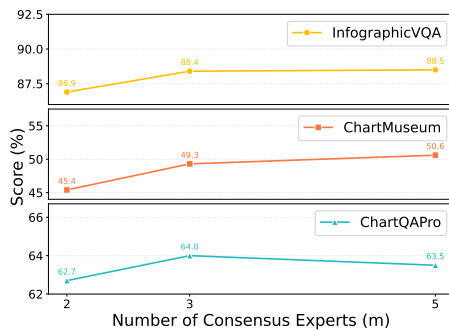
435 4.5 ABLATION STUDY

437 To better understand the effectiveness of SV, we conduct ablation studies on information-intensive
 438 benchmarks to analyze the impact of individual components. In these experiments, the reasoning
 439 baseline refers to the best-performing draft expert in our pool for each benchmark (Table 1).

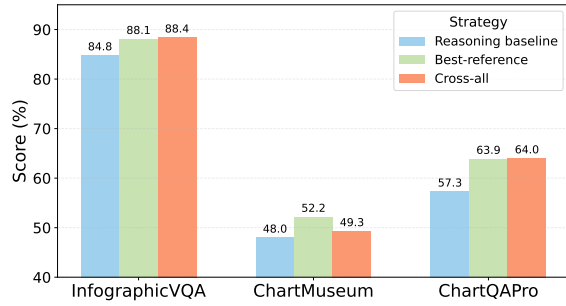
440 **Number of Draft Experts.** Our setting with $m = 3$ draft experts yields a favorable trade-off
 441 between accuracy and efficiency, as it determines the number of reasoning paths forwarded to the
 442 verdict. As shown in Figure 5, we observe that the performance improves nearly linearly up to three
 443 draft experts and then saturates, while inference cost grows roughly linearly with m .

444 **Consensus Expert Selection Strategy.** We confirm the effectiveness of our cross-all selection strategy
 445 by comparing it with a best-reference strategy. In the best-reference variant, the top-performing
 446 draft expert serves as reference and the two most consistent experts are selected with it. While
 447 best-reference is expected to be the strongest criterion, cross-all achieves comparable gains while
 448 remaining reference-free (Figure 6).

449 **Selection Criteria.** Selecting consensus-based experts consistently improves performance, while
 450 divergent selection can even fall below the single-draft reasoning baseline (Figure 7). These results
 451 support that, for information-intensive tasks, consensus-based selection more reliably identifies the
 452 correct reasoning path than enforced diversity.



464 Figure 5: Ablations on the number of draft
 465 experts m .
 466



464 Figure 6: Ablations on different consensus expert se-
 465 lecting strategies.
 466

467 **Impact of Verdict Stage.** The verdict stage yields higher performance than majority voting across
 468 information-intensive benchmarks (Figure 8). Notably, majority voting with all five **candidate models**
 469 performs comparably as majority voting with three draft experts, consistent with our finding that
 470 consensus selection can match the performance of all drafts at a lower cost (Table 5). SV further
 471 surpasses both by leveraging the verdict’s error correction ability, successfully capturing minority-
 472 correct cases that majority voting discards (Figure 4 and Figure 3).

473 **Beyond majority voting, SV consistently outperforms a strong LMM-as-a-Judge baseline (LLaVA-
 474 Critic-72B (Xiong et al., 2025)) by 4.9–11.9% (Figure 8).** In this setting, LLaVA-Critic scores or
 475 ranks the same draft experts selected by SV and outputs the single best candidate. This advantage is
 476 attributed to SV’s synthesis-based verdict, which cross-checks and integrates complementary factual
 477 cues across multiple trajectories, rather than relying on selecting one trajectory that may be favored
 478 by reasoning style. Detailed ablations with LLaVA-Critic are provided in Appendix G.

479 **Choice of Verdict Textual Input.** Providing full reasoning paths to the verdict yields substantially
 480 better performance than passing only final answers (Table 3), with improvements of 15% on Info-
 481 graphicVQA, and 4.8% on ChartQapro. These results highlight that rich contextual evidence is
 482 essential for the verdict to recover correct reasoning, whereas final predictions alone are insufficient.

483 **Choice of Verdict Scale.** Using a large verdict model yields stronger gains than a small verdict
 484 model. We evaluate three strong small verdicts (i.e., GLM-4.1V-9B-Thinking, MiMO-VL-7B-RL,
 485 Qwen2.5-VL-7B-Instruct), and all of them underperform SV across benchmarks (Table 4). Notably,

486 the small reasoning verdicts generate 60–200x more output tokens yet still yield weaker performance,
 487 indicating worse cost-efficiency trade-offs (details in Appendix C). The results validate SV’s design
 488 principle of invoking a strong verdict only once to achieve robust and efficient error correction.
 489

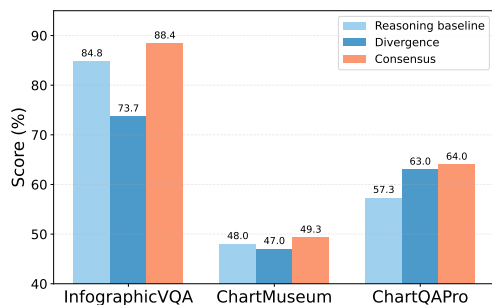


Figure 7: Ablations on selection criteria.

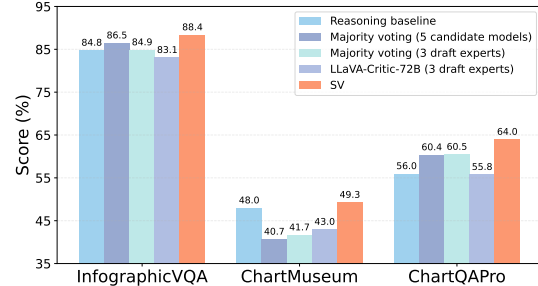


Figure 8: Performance comparison on SV, majority voting and LLaVA-Critic with different model sets.

Table 3: Ablations on verdict textual input.

Textual input	InfographicVQA ANLS	ChartQAPro Acc
Reasoning baseline	84.8	57.3
Answers only	73.4	59.2
Reasoning paths (SV)	88.4	64.0

Table 4: Ablations on verdict scale.

Verdict Choice	InfographicVQA ANLS	ChartMuseum Acc	ChartQAPro Acc
Reasoning baseline	84.8	48.0	57.3
GLM-4.1V-9B-Thinking Verdict	84.7	48.0	59.4
MiMO-VL-RL-7B Verdict	85.4	46.9	60.3
Owen2.5-VL-Instruct 7B Verdict	84.1	47.1	57.2
GPT-4o Verdict	88.4	49.3	64.0

4.6 COST-EFFICIENCY ANALYSIS

511 We quantify SV’s cost-efficiency by comparing it against large reasoning model baselines, including
 512 GPT-4o and o1. As described in Section 3.3, SV achieves cost-efficiency through its verdict stage by
 513 concentrating computation in prefill and substantially reducing expensive autoregressive decoding.

514 As shown in Table 5 and 6, SV consistently improves over GPT-4o by 6.6–12.0% across datasets
 515 while maintaining comparable cost. Compared with o1, SV attains substantially better performance
 516 on InfographicVQA and ChartQAPro and comparable performance on ChartMuseum while requir-
 517 ing only 15–26% of o1’s cost. These results confirm that SV delivers markedly superior cost-
 518 efficiency, achieving and even outperforming o1-level performance with lower computational cost.

Table 5: Performance on 1000 randomly sampled test instances per benchmark.

Method	InfographicVQA	ChartMuseum	ChartQAPro
GPT-4o	76.3	42.7	51.7
GPT-o1	77.8	50.6	58.8
SV w/ GPT-4o Verdict	88.3	49.3	63.4

Table 6: Average inference API cost per sample across benchmarks.

Method	InfographicVQA	ChartMuseum	ChartQAPro
GPT-4o	\$0.0038	\$0.0213	\$0.0210
GPT-o1	\$0.0263	\$0.0663	\$0.0478
SV w/ GPT-4o Verdict	\$0.0068	\$0.0109	\$0.0071

5 CONCLUSION

534 This paper introduces Speculative Verdict (SV), a training-free framework to address challenges
 535 of information-intensive visual reasoning. Inspired by speculative decoding, SV repositions large
 536 models as efficient synthesizers rather than computationally expensive step-by-step reasoners. By
 537 integrating diverse reasoning paths from lightweight experts, the verdict can distinguish informa-
 538 tive cues and recover correctness from structured errors. Experiments show that SV consistently
 539 outperforms strong proprietary, open-source, and tool-driven methods, establishing a cost-efficient
 paradigm for reasoning on information-intensive images.

540 **6 ETHICS STATEMENT**
541542 All authors have read and commit to adhering to the ICLR Code of Ethics. This work does not in-
543 volve human subjects, sensitive personal data, biometrics, or medical information. All datasets used
544 are publicly available under permissible licenses and are not privacy-sensitive. We recognize that
545 any automated reasoning system may produce incorrect or misleading outputs. To ensure responsi-
546 ble use, we emphasize that our method is intended for research and analysis rather than deployment
547 in high-stakes settings. Users are encouraged to verify model outputs and apply human oversight
548 when necessary. We take full responsibility for all reported results, analyses, and claims, and we
549 welcome community scrutiny and feedback.
550551 **7 REPRODUCIBILITY STATEMENT**
552553 To support reproducibility, we provide comprehensive implementation details throughout our paper.
554 Key experimental configurations, such as draft expert selection, consensus scoring computation,
555 and verdict model specifications, are documented in Section 3.4 and Section 4.1. Detailed prompt
556 templates are presented in Appendix M. The supplementary material includes anonymized source
557 code to further clarify the implementation steps and enable faithful reproduction of our results.
558559 **REFERENCES**
560561 Manoj Acharya, Kushal Kafle, and Christopher Kanan. Tallyqa: Answering complex counting
562 questions. In *Proceedings of the AAAI conference on artificial intelligence*, volume 33, pp. 8076–
563 8084, 2019.564 Xiang An, Yin Xie, Kaicheng Yang, Wenkang Zhang, Xiuwei Zhao, Zheng Cheng, Yirui Wang,
565 Songcen Xu, Changrui Chen, Chunsheng Wu, et al. Llava-onevision-1.5: Fully open framework
566 for democratized multimodal training. *arXiv preprint arXiv:2509.23661*, 2025.568 Shuai Bai, Keqin Chen, Xuejing Liu, Jialin Wang, Wenbin Ge, Sibo Song, Kai Dang, Peng Wang,
569 Shijie Wang, Jun Tang, et al. Qwen2. 5-vl technical report. *arXiv preprint arXiv:2502.13923*,
570 2025.572 Guo Chen, Zhiqi Li, Shihao Wang, Jindong Jiang, Yicheng Liu, Lidong Lu, De-An Huang, Wonmin
573 Byeon, Matthieu Le, Tuomas Rintamaki, et al. Eagle 2.5: Boosting long-context post-training for
574 frontier vision-language models. *arXiv preprint arXiv:2504.15271*, 2025.575 Xinyun Chen, Renat Akositov, Uri Alon, Jie Ren, Kefan Xiao, Pengcheng Yin, Sushant Prakash,
576 Charles Sutton, Xuezhi Wang, and Denny Zhou. Universal self-consistency for large language
577 model generation. *arXiv preprint arXiv:2311.17311*, 2023.579 Cheng Cui, Ting Sun, Manhui Lin, Tingquan Gao, Yubo Zhang, Jiaxuan Liu, Xueqing Wang,
580 Zelun Zhang, Changda Zhou, Hongen Liu, et al. Paddleocr 3.0 technical report. *arXiv preprint*
581 *arXiv:2507.05595*, 2025.583 Yue Fan, Xuehai He, Diji Yang, Kaizhi Zheng, Ching-Chen Kuo, Yuting Zheng, Sravana Jyothi
584 Narayananaraju, Xinze Guan, and Xin Eric Wang. Grit: Teaching mllms to think with images.
585 *arXiv preprint arXiv:2505.15879*, 2025.586 Chaoyou Fu, Yi-Fan Zhang, Shukang Yin, Bo Li, Xinyu Fang, Sirui Zhao, Haodong Duan, Xing
587 Sun, Ziwei Liu, Liang Wang, et al. Mme-survey: A comprehensive survey on evaluation of
588 multimodal llms. *arXiv preprint arXiv:2411.15296*, 2024.590 Jiale Fu, Yuchu Jiang, Junkai Chen, Jiaming Fan, Xin Geng, and Xu Yang. Fast large language
591 model collaborative decoding via speculation. *arXiv preprint arXiv:2502.01662*, 2025a.592 Yichao Fu, Rui Ge, Zelei Shao, Zhijie Deng, and Hao Zhang. Scaling speculative decoding with
593 lookahead reasoning. *arXiv preprint arXiv:2506.19830*, 2025b.

594 Wentao Ge, Shunian Chen, Hardy Chen, Nuo Chen, Junying Chen, Zhihong Chen, Wenya Xie,
 595 Shuo Yan, ChenghaoZhu ChenghaoZhu, Ziyue Lin, et al. Mllm-bench: evaluating multimodal
 596 llms with per-sample criteria. In *Proceedings of the 2025 Conference of the Nations of the Amer-*
 597 *icas Chapter of the Association for Computational Linguistics: Human Language Technologies*
 598 (*Volume 1: Long Papers*), pp. 4951–4974, 2025.

599 Daya Guo, Dejian Yang, Haowei Zhang, Junxiao Song, Ruoyu Zhang, Runxin Xu, Qihao Zhu,
 600 Shirong Ma, Peiyi Wang, Xiao Bi, et al. Deepseek-r1: Incentivizing reasoning capability in llms
 601 via reinforcement learning. *arXiv preprint arXiv:2501.12948*, 2025.

602 Yushi Hu, Weijia Shi, Xingyu Fu, Dan Roth, Mari Ostendorf, Luke Zettlemoyer, Noah A Smith, and
 603 Ranjay Krishna. Visual sketchpad: Sketching as a visual chain of thought for multimodal lan-
 604 guage models. *Advances in Neural Information Processing Systems*, 37:139348–139379, 2024.

605 Wenzuan Huang, Bohan Jia, Zijie Zhai, Shaosheng Cao, Zheyu Ye, Fei Zhao, Zhe Xu, Yao Hu, and
 606 Shaohui Lin. Vision-r1: Incentivizing reasoning capability in multimodal large language models.
 607 *arXiv preprint arXiv:2503.06749*, 2025.

608 Aaron Hurst, Adam Lerer, Adam P Goucher, Adam Perelman, Aditya Ramesh, Aidan Clark, AJ Os-
 609 trow, Akila Welihinda, Alan Hayes, Alec Radford, et al. Gpt-4o system card. *arXiv preprint*
 610 *arXiv:2410.21276*, 2024.

611 Aaron Jaech, Adam Kalai, Adam Lerer, Adam Richardson, Ahmed El-Kishky, Aiden Low, Alec
 612 Helyar, Aleksander Madry, Alex Beutel, Alex Carney, et al. Openai o1 system card. *arXiv*
 613 *preprint arXiv:2412.16720*, 2024.

614 Fucai Ke, Joy Hsu, Zhixi Cai, Zixian Ma, Xin Zheng, Xindi Wu, Sukai Huang, Weiqing Wang,
 615 Pari Delir Haghghi, Gholamreza Haffari, Ranjay Krishna, Jiajun Wu, and Hamid Rezatofighi.
 616 Explain before you answer: A survey on compositional visual reasoning, 2025.

617 Yaniv Leviathan, Matan Kalman, and Yossi Matias. Fast inference from transformers via speculative
 618 decoding. In *International Conference on Machine Learning*, pp. 19274–19286. PMLR, 2023.

619 Bo Li, Yuanhan Zhang, Dong Guo, Renrui Zhang, Feng Li, Hao Zhang, Kaichen Zhang, Peiyuan
 620 Zhang, Yanwei Li, Ziwei Liu, et al. Llava-onevision: Easy visual task transfer. *arXiv preprint*
 621 *arXiv:2408.03326*, 2024.

622 Dawei Li, Bohan Jiang, Liangjie Huang, Alimohammad Beigi, Chengshuai Zhao, Zhen Tan, Amrita
 623 Bhattacharjee, Yuxuan Jiang, Canyu Chen, Tianhao Wu, et al. From generation to judgment: Op-
 624 portunities and challenges of llm-as-a-judge. In *Proceedings of the 2025 Conference on Empirical*
 625 *Methods in Natural Language Processing*, pp. 2757–2791, 2025a.

626 Lei Li, Yuancheng Wei, Zhihui Xie, Xuqing Yang, Yifan Song, Peiyi Wang, Chenxin An, Tianyu
 627 Liu, Sujian Li, Bill Yuchen Lin, et al. Vl-rewardbench: A challenging benchmark for vision-
 628 language generative reward models. In *Proceedings of the Computer Vision and Pattern Recog-*
 629 *nition Conference*, pp. 24657–24668, 2025b.

630 Zongxia Li, Xiyang Wu, Hongyang Du, Fuxiao Liu, Huy Nghiem, and Guangyao Shi. A survey of
 631 state of the art large vision language models: Alignment, benchmark, evaluations and challenges.
 632 *arXiv preprint arXiv:2501.02189*, 2025c.

633 Baohao Liao, Yuhui Xu, Hanze Dong, Junnan Li, Christof Monz, Silvio Savarese, Doyen Sahoo, and
 634 Caiming Xiong. Reward-guided speculative decoding for efficient llm reasoning. *arXiv preprint*
 635 *arXiv:2501.19324*, 2025.

636 Pan Lu, Hritik Bansal, Tony Xia, Jiacheng Liu, Chunyuan Li, Hannaneh Hajishirzi, Hao Cheng, Kai-
 637 Wei Chang, Michel Galley, and Jianfeng Gao. Mathvista: Evaluating mathematical reasoning of
 638 foundation models in visual contexts. *arXiv preprint arXiv:2310.02255*, 2023.

639 Shiyin Lu, Yang Li, Yu Xia, Yuwei Hu, Shanshan Zhao, Yanqing Ma, Zhichao Wei, Yinglun Li,
 640 Lunhao Duan, Jianshan Zhao, et al. Ovis2. 5 technical report. *arXiv preprint arXiv:2508.11737*,
 641 2025.

648 Xinyu Ma, Ziyang Ding, Zhicong Luo, Chi Chen, Zonghao Guo, Derek F Wong, Xiaoyi Feng,
 649 and Maosong Sun. Deepperception: Advancing r1-like cognitive visual perception in mllms for
 650 knowledge-intensive visual grounding. *arXiv preprint arXiv:2503.12797*, 2025.

651

652 Ahmed Masry, Mohammed Saidul Islam, Mahir Ahmed, Aayush Bajaj, Firoz Kabir, Aaryaman
 653 Kartha, Md Tahmid Rahman Laskar, Mizanur Rahman, Shadikur Rahman, Mehrad Shahmoham-
 654 madi, et al. Chartqapro: A more diverse and challenging benchmark for chart question answering.
 655 *arXiv preprint arXiv:2504.05506*, 2025.

656 Minesh Mathew, Viraj Bagal, Rubén Pérez Tito, Dimosthenis Karatzas, Ernest Valveny, and C. V
 657 Jawahar. Infographiccvqa. *arXiv preprint arXiv:2104.12756*, 2021.

658

659 Chancharik Mitra, Brandon Huang, Trevor Darrell, and Roei Herzig. Compositional chain-of-
 660 thought prompting for large multimodal models. In *Proceedings of the IEEE/CVF Conference*
 661 *on Computer Vision and Pattern Recognition*, pp. 14420–14431, 2024.

662 Rui Pan, Yinwei Dai, Zhihao Zhang, Gabriele Oliaro, Zhihao Jia, and Ravi Netravali. Specrea-
 663 son: Fast and accurate inference-time compute via speculative reasoning. *arXiv preprint*
 664 *arXiv:2504.07891*, 2025.

665 Ji Qi, Ming Ding, Weihan Wang, Yushi Bai, Qingsong Lv, Wenyi Hong, Bin Xu, Lei Hou, Juanzi Li,
 666 Yuxiao Dong, et al. Cogcom: A visual language model with chain-of-manipulations reasoning.
 667 *arXiv preprint arXiv:2402.04236*, 2024.

668

669 Jianing Qi, Xi Ye, Hao Tang, Zhigang Zhu, and Eunsol Choi. Learning to reason across parallel
 670 samples for llm reasoning. *arXiv preprint arXiv:2506.09014*, 2025.

671 Hao Shao, Shengju Qian, Han Xiao, Guanglu Song, Zhuofan Zong, Letian Wang, Yu Liu, and Hong-
 672 sheng Li. Visual cot: Advancing multi-modal language models with a comprehensive dataset and
 673 benchmark for chain-of-thought reasoning. *Advances in Neural Information Processing Systems*,
 674 37:8612–8642, 2024.

675

676 Haozhan Shen, Kangjia Zhao, Tiancheng Zhao, Ruochen Xu, Zilun Zhang, Mingwei Zhu, and Jian-
 677 wei Yin. Zoomeye: Enhancing multimodal llms with human-like zooming capabilities through
 678 tree-based image exploration. *arXiv preprint arXiv:2411.16044*, 2024.

679

680 Alex Su, Haozhe Wang, Weiming Ren, Fangzhen Lin, and Wenhu Chen. Pixel reasoner: In-
 681 centivizing pixel-space reasoning with curiosity-driven reinforcement learning. *arXiv preprint*
 682 *arXiv:2505.15966*, 2025a.

683

684 Zhaochen Su, Peng Xia, Hangyu Guo, Zhenhua Liu, Yan Ma, Xiaoye Qu, Jiaqi Liu, Yanshu Li,
 685 Kaide Zeng, Zhengyuan Yang, et al. Thinking with images for multimodal reasoning: Founda-
 686 tions, methods, and future frontiers. *arXiv preprint arXiv:2506.23918*, 2025b.

687

688 Liyan Tang, Grace Kim, Xinyu Zhao, Thom Lake, Wenxuan Ding, Fangcong Yin, Prasann Singhal,
 689 Manya Wadhwa, Zeyu Leo Liu, Zayne Sprague, et al. Chartmuseum: Testing visual reasoning
 690 capabilities of large vision-language models. *arXiv preprint arXiv:2505.13444*, 2025.

691

692 Gemma Team, Aishwarya Kamath, Johan Ferret, Shreya Pathak, Nino Vieillard, Ramona Merhej,
 693 Sarah Perrin, Tatiana Matejovicova, Alexandre Ramé, Morgane Rivière, et al. Gemma 3 technical
 694 report. *arXiv preprint arXiv:2503.19786*, 2025a.

695

696 V Team, Wenyi Hong, Wenmeng Yu, Xiaotao Gu, Guo Wang, Guobing Gan, Haomiao Tang, Jiale
 697 Cheng, Ji Qi, Junhui Ji, Lihang Pan, Shuaiqi Duan, Weihan Wang, Yan Wang, Yean Cheng,
 698 Zehai He, Zhe Su, Zhen Yang, Ziyang Pan, Aohan Zeng, Baoxu Wang, Bin Chen, Boyan Shi,
 699 Changyu Pang, Chenhui Zhang, Da Yin, Fan Yang, Guoqing Chen, Jiazheng Xu, Jiale Zhu, Jiali
 700 Chen, Jing Chen, Jinhao Chen, Jinghao Lin, Jinjiang Wang, Junjie Chen, Leqi Lei, Letian Gong,
 701 Leyi Pan, Mingdao Liu, Mingde Xu, Mingzhi Zhang, Qinkai Zheng, Sheng Yang, Shi Zhong,
 702 Shiyu Huang, Shuyuan Zhao, Siyan Xue, Shangqin Tu, Shengbiao Meng, Tianshu Zhang, Tianwei
 703 Luo, Tianxiang Hao, Tianyu Tong, Wenkai Li, Wei Jia, Xiao Liu, Xiaohan Zhang, Xin Lyu,
 704 Xinyue Fan, Xuancheng Huang, Yanling Wang, Yadong Xue, Yanfeng Wang, Yanzi Wang, Yifan
 705 An, Yifan Du, Yiming Shi, Yiheng Huang, Yilin Niu, Yuan Wang, Yuanchang Yue, Yuchen Li,
 706 Yutao Zhang, Yuting Wang, Yu Wang, Yuxuan Zhang, Zhao Xue, Zhenyu Hou, Zhengxiao Du,

702 Zihan Wang, Peng Zhang, Debing Liu, Bin Xu, Juanzi Li, Minlie Huang, Yuxiao Dong, and Jie
 703 Tang. Glm-4.5v and glm-4.1v-thinking: Towards versatile multimodal reasoning with scalable
 704 reinforcement learning, 2025b. URL <https://arxiv.org/abs/2507.01006>.

705 Weiyun Wang, Zhangwei Gao, Lixin Gu, Hengjun Pu, Long Cui, Xingguang Wei, Zhaoyang Liu,
 706 Linglin Jing, Shenglong Ye, Jie Shao, et al. Internvl3. 5: Advancing open-source multimodal
 707 models in versatility, reasoning, and efficiency. *arXiv preprint arXiv:2508.18265*, 2025a.

708 Wenbin Wang, Liang Ding, Minyan Zeng, Xiabin Zhou, Li Shen, Yong Luo, Wei Yu, and Dacheng
 709 Tao. Divide, conquer and combine: A training-free framework for high-resolution image percep-
 710 tion in multimodal large language models. In *Proceedings of the AAAI Conference on Artificial
 711 Intelligence*, volume 39, pp. 7907–7915, 2025b.

712 Wenbin Wang, Yongcheng Jing, Liang Ding, Yingjie Wang, Li Shen, Yong Luo, Bo Du, and
 713 Dacheng Tao. Retrieval-augmented perception: High-resolution image perception meets visual
 714 rag. *arXiv preprint arXiv:2503.01222*, 2025c.

715 Jason Wei, Xuezhi Wang, Dale Schuurmans, Maarten Bosma, Fei Xia, Ed Chi, Quoc V Le, Denny
 716 Zhou, et al. Chain-of-thought prompting elicits reasoning in large language models. *Advances in
 717 neural information processing systems*, 35:24824–24837, 2022.

718 Penghao Wu and Saining Xie. V?: Guided visual search as a core mechanism in multimodal llms.
 719 In *Proceedings of the IEEE/CVF Conference on Computer Vision and Pattern Recognition*, pp.
 720 13084–13094, 2024.

721 Yilin Wu, Ran Tian, Gokul Swamy, and Andrea Bajcsy. From foresight to forethought: Vlm-in-the-
 722 loop policy steering via latent alignment. *arXiv preprint arXiv:2502.01828*, 2025.

723 Heming Xia, Zhe Yang, Qingxiu Dong, Peiyi Wang, Yongqi Li, Tao Ge, Tianyu Liu, Wenjie Li, and
 724 Zhifang Sui. Unlocking efficiency in large language model inference: A comprehensive survey
 725 of speculative decoding. *arXiv preprint arXiv:2401.07851*, 2024.

726 LLM-Core-Team Xiaomi. Mimo-vl technical report, 2025. URL <https://arxiv.org/abs/2506.03569>.

727 Tianyi Xiong, Xiyao Wang, Dong Guo, Qinghao Ye, Haoqi Fan, Quanquan Gu, Heng Huang, and
 728 Chunyuan Li. Llava-critic: Learning to evaluate multimodal models. In *Proceedings of the
 729 Computer Vision and Pattern Recognition Conference*, pp. 13618–13628, 2025.

730 Guowei Xu, Peng Jin, Ziang Wu, Hao Li, Yibing Song, Lichao Sun, and Li Yuan. Llava-cot:
 731 Let vision language models reason step-by-step. In *Proceedings of the IEEE/CVF International
 732 Conference on Computer Vision*, pp. 2087–2098, 2025.

733 Wang Yang, Xiang Yue, Vipin Chaudhary, and Xiaotian Han. Speculative thinking: Enhanc-
 734 ing small-model reasoning with large model guidance at inference time. *arXiv preprint
 735 arXiv:2504.12329*, 2025a.

736 Zeyuan Yang, Xueyang Yu, Delin Chen, Maohao Shen, and Chuang Gan. Machine mental imagery:
 737 Empower multimodal reasoning with latent visual tokens. *arXiv preprint arXiv:2506.17218*,
 738 2025b.

739 Chen Zhang, Zhuorui Liu, and Dawei Song. Beyond the speculative game: A survey of speculative
 740 execution in large language models. *arXiv preprint arXiv:2404.14897*, 2024.

741 Jiarui Zhang, Mahyar Khayatkhoei, Prateek Chhikara, and Filip Ilievski. Mllms know where to
 742 look: Training-free perception of small visual details with multimodal llms. *arXiv preprint
 743 arXiv:2502.17422*, 2025a.

744 Xinlu Zhang, Yujie Lu, Weizhi Wang, An Yan, Jun Yan, Lianke Qin, Heng Wang, Xifeng Yan,
 745 William Yang Wang, and Linda Ruth Petzold. Gpt-4v (ision) as a generalist evaluator for vision-
 746 language tasks. *arXiv preprint arXiv:2311.01361*, 2023.

756 Xintong Zhang, Zhi Gao, Bofei Zhang, Pengxiang Li, Xiaowen Zhang, Yang Liu, Tao Yuan, Yuwei
757 Wu, Yunde Jia, Song-Chun Zhu, et al. Chain-of-focus: Adaptive visual search and zooming for
758 multimodal reasoning via rl. *arXiv preprint arXiv:2505.15436*, 2025b.

759
760 Wenting Zhao, Pranjal Aggarwal, Swarnadeep Saha, Asli Celikyilmaz, Jason Weston, and Ilia Ku-
761 likov. The majority is not always right: Rl training for solution aggregation. *arXiv preprint*
762 *arXiv:2509.06870*, 2025.

763 Ziwei Zheng, Michael Yang, Jack Hong, Chenxiao Zhao, Guohai Xu, Le Yang, Chao Shen, and
764 Xing Yu. Deepeyes: Incentivizing” thinking with images” via reinforcement learning. *arXiv*
765 *preprint arXiv:2505.14362*, 2025.

766 Jinguo Zhu, Weiyun Wang, Zhe Chen, Zhaoyang Liu, Shenglong Ye, Lixin Gu, Hao Tian, Yuchen
767 Duan, Weijie Su, Jie Shao, et al. Internvl3: Exploring advanced training and test-time recipes for
768 open-source multimodal models. *arXiv preprint arXiv:2504.10479*, 2025.

770

771

772

773

774

775

776

777

778

779

780

781

782

783

784

785

786

787

788

789

790

791

792

793

794

795

796

797

798

799

800

801

802

803

804

805

806

807

808

809

810 A DATASET STATISTICS
811

812 Table 7 reports the statistics of the four **major** evaluation benchmarks. All benchmarks are based on
813 **real-world images** rather than synthetic renderings, ensuring the authenticity and diversity of the
814 evaluation setting. In particular, InfographicVQA, ChartMuseum, and ChartQAPro are information-
815 intensive benchmarks: they contain thousands of images and questions with dense textual and nu-
816 matical content, collected from diverse sources spanning 2594, 157, and 184 distinct web domains
817 respectively (Mathew et al., 2021; Tang et al., 2025; Masry et al., 2025). This diversity reduces
818 source bias and reflects practical challenges in multimodal reasoning.

819 HR-Bench 4K is used primarily to evaluate the generalization of **SV**, serving as a high-resolution
820 benchmark with average sizes exceeding 4000×3500 (Wang et al., 2025b). **Meanwhile**, one of our
821 main benchmarks, InfographicVQA, also exhibits high-resolution characteristics. In particular, it
822 contains **many** images where diagrams span large vertical layouts (see the case in Figure 3), which
823 further compounds the difficulty of grounding and multi-hop reasoning across dispersed regions.

824
825 Table 7: Statistics of the evaluation benchmarks. We report the number of images and questions, as
826 well as the average image resolution (width \bar{W} and height \bar{H}).

Dataset	Real vs. Synthetic	#Images	#Questions	\bar{W}	\bar{H}
InfographicVQA (test)	Real	3288	579	1092	2771
ChartMuseum (test)	Real	1000	818	1551	1213
ChartQAPro	Real	1948	1341	1194	986
HR-Bench 4K	Real	800	200	4024	3503

834 B ADDITIONAL RELATED WORK
835

836
837 **Large Language Model Ensemble.** Majority voting aggregates answers by frequency, but fails
838 when the correct solution is produced by a minority. Universal Self-Consistency (Chen et al.,
839 2023) mitigates this failure mode by prompting the LLM to select the most consistent candidate
840 across samples. Further, learned aggregators read multiple rationales and synthesize them to recover
841 minority-correct information (Qi et al., 2025; Zhao et al., 2025). However, these approaches focus on
842 text-only ensembling. In vision-language reasoning, supervision of ensembling is not cost-effective
843 since multimodal complexity requires costly, fine-grained annotations.

844 C ADDITIONAL COST-EFFICIENCY ANALYSIS
845846 C.1 AVERAGE API COST OF SV WITH GPT-4O VERDICT
847

848 Table 8 reports the average inference cost of invoking GPT-4o as the verdict model per sample across
849 benchmarks. Costs are estimated using the official GPT-4o pricing (version gpt-4o-2024-08-06) as
850 of September 2025. The small variation across benchmarks is mainly attributed to differences in
851 reasoning path length, as more challenging tasks typically induce more complex reasoning. Overall,
852 the inference cost of using GPT-4o as the verdict is under \$0.011 per sample across all benchmarks.

853
854 Table 8: Average inference cost of GPT-4o as verdict per sample across benchmarks. Costs are
855 computed using GPT-4o (gpt-4o-2024-08-06) pricing by **November** 2025.

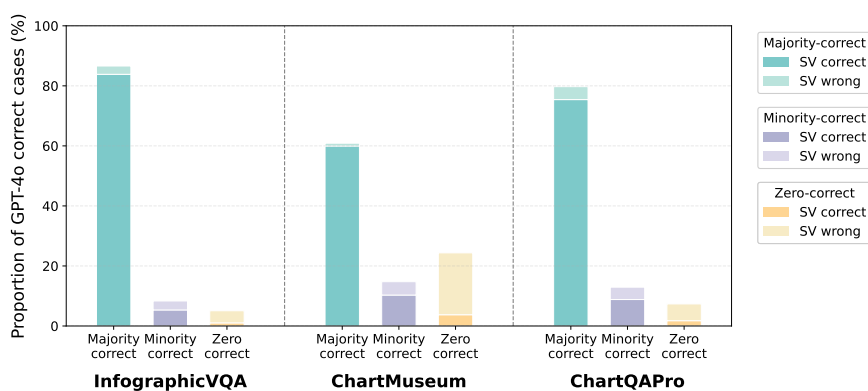
Dataset	GPT-4o cost per sample
InfographicVQA	\$0.0068
ChartMuseum	\$0.0109
ChartQAPro	\$0.0071
HR-Bench 4K	\$0.0044

864 **C.2 AVERAGE OUTPUT TOKENS ACROSS VERDICTS**
865866 To compare the token efficiency of replacing the large verdict with smaller models, we keep the
867 draft stage identical and substitute the verdict with different draft models. All verdict models are
868 prompted to output only the final answer, and their performances are reported in Table 4 in the main
869 paper.870 As shown in Table 9, the small reasoning models, GLM-4.1V-9B-Thinking and MiMO-VL-7B-RL,
871 generate 60–200x more output tokens than GPT-4o, yet still underperform SV. This highlights SV’s
872 advantage: using a strong verdict once for compact verification and synthesis is substantially more
873 token-efficient than relying on smaller verdicts that require long autoregressive reasoning to reach a
874 decision.875 **Table 9: Average verdict output tokens per sample across benchmarks under different verdicts.**
876

Verdict model	InfographicVQA	ChartMuseum	ChartQAPro
GLM-4.1V-9B-Thinking	272.1	604.5	440.5
MiMO-VL-7B-RL	183.2	368.2	378.1
Qwen2.5-VL-7B-Instruct	3.3	3.4	2.8
GPT-4o (SV)	2.7	3.0	2.2

877 **D SUPPLEMENTARY RECOVERY ANALYSIS ON INFORMATION-INTENSIVE
878 BENCHMARKS**
879880 Table 10 and Figure 11 show the detailed recovery statistics across benchmarks with GPT-4o as
881 verdict. We break down SV’s performance by expert correctness: (i) cases where the majority of
882 draft experts are correct (majority-correct), (ii) cases where only a minority are correct (minority-
883 correct), (iii) cases where none are correct (zero-correct). While the main paper focuses on the
884 GPT-4o’s error cases to isolate SV’s effectiveness, we provide the full results here for completeness.
885 Notably, in the zero-correct setting, recovery occurs rarely (2.6–24%), but it demonstrates verdict’s
886 surprising ability to infer the correct answer by synthesizing signal from entirely noisy reasoning.
887888 **Table 10: Recovery accuracy (%) with GPT-4o as verdict. Results are conditioned on whether GPT-
889 4o itself can produce the correct answer.**
890

Dataset	GPT-4o Correct			GPT-4o Wrong		
	Majority-correct	Minority-correct	Zero-correct	Majority-correct	Minority-correct	Zero-correct
InfographicVQA	96.81	64.13	20.54	93.30	53.42	4.44
ChartMuseum	98.46	69.84	15.38	89.92	47.71	2.69
ChartQAPro	94.59	68.18	24.00	85.25	48.43	2.86

915 **Table 11: SV’s correction ability on verdict’s correct cases (GPT-4o as verdict), complementary to
916 its error cases in Figure 4.**
917

918
919 Table 12: Results on test sets of InfographicVQA with 7–9B draft experts. We compare SV against
920 closed-source VLMs, open-source VLMs, and tool-driven methods. \dagger denotes results reported in
921 the original papers; all other results are reproduced by us. The best results for each benchmark are
922 highlighted in **bold** and the second-best results are underlined.

Model	Param Size	InfographicVQA ANLS
<i>Closed-source VLMs</i>		
GPT-4o	–	76.5
GPT-4o-mini	–	67.2
<i>Open-source VLMs</i>		
Qwen2.5-VL-Instruct	7B	79.8
LLaVA-OneVision-1.5	8B	70.3
InternVL3	8B	72.3
Eagle 2.5	8B	74.5
Ovis2.5	9B	81.7
<i>Tool-driven method</i>		
DeepEyes	7B	75.5
Pixel-Reasoner	7B	<u>84.0</u> \dagger
SV w/ GPT-4o Verdict	–	86.3
Δ (vs. GPT-4o)	–	+9.8

938
939 Table 13: Results on test sets on InfographicVQA with 2–4B draft experts. Same evaluation and
940 marking conventions as Table 12.

Model	Param Size	InfographicVQA ANLS
<i>Closed-source VLMs</i>		
GPT-4o	–	76.5
GPT-4o-mini	–	67.2
<i>Open-source VLMs</i>		
Qwen2.5-VL-Instruct	3B	64.9
LLaVA-OneVision-1.5	4B	67.1
InternVL3.5	4B	74.4
Gemma 3	4B	36.0
Ovis2.5	2B	75.0
<i>Tool-driven method</i>		
DeepEyes	7B	75.5
Pixel-Reasoner	7B	<u>84.0</u> \dagger
SV w/ GPT-4o Verdict	–	84.5
Δ (vs. GPT-4o)	–	+8.0

E ABLATION STUDY ON MODEL POOL COMPOSITIONS

959 Beyond the fixed model pool used in the main experiments, we further examine SV’s generaliz-
960 ability across different model pool compositions by testing on pools with varying model sizes and
961 capabilities. The results show that SV successfully leverages reasoning paths from lightweight mod-
962 els, delivering strong performance while maintaining cost efficiency.

963 **Evaluation with 7-9B Model Pool (Non-reasoning).** SV maintains its effectiveness when replacing
964 reasoning models with faster non-reasoning alternatives. Specifically, we replace the two reasoning
965 models in our original pool (i.e., GLM-4.1V-9B-Thinking (Team et al., 2025b) and MiMO-VL-7B-
966 RL (Xiaomi, 2025)) with non-reasoning models (i.e., LLaVA-OneVision-1.5-8B (An et al., 2025),
967 and Eagle 2.5-8B (Chen et al., 2025)), while keeping the remaining three models unchanged. While
968 these substitutes sacrifice some reasoning capability, they enable faster inference. As shown in
969 Table 12, with GPT-4o as verdict, SV achieves 86.3% on InfographicVQA under this configuration,
970 surpassing all baselines. Notably, SV surpasses the best draft expert by 4.6% and improves over
971 GPT-4o by 9.8%. These results demonstrate that SV achieves strong performance by integrating
972 reasoning paths from individually weaker but faster models.

972 **Evaluation with 2-4B Model Pool.** We also evaluate SV on an even smaller model pool consisting
 973 of 2-4B models: Qwen2.5-VL-3B-Instruct (Bai et al., 2025), LLaVA-OneVision-1.5-4B (An
 974 et al., 2025), InternVL3.5-4B (Wang et al., 2025a), Gemma 3-4B (Team et al., 2025a), and Ovis2.5-
 975 2B (Lu et al., 2025). As shown in the Table 13, with GPT-4o as verdict, SV achieves 84.5% on Info-
 976 graphicVQA, surpassing the best draft expert by 9.5% and yielding an 8% gain over GPT-4o. This
 977 demonstrates SV’s ability to extract effective collective reasoning even from significantly weaker
 978 individual models, confirming the robustness of our paradigm across varying model scales.

980 F ANALYSIS OF CONSENSUS SELECTION MECHANISM

982 This section provides a detailed analysis of our consensus expert selection mechanism, addressing
 983 three aspects: (1) selection frequency distribution, (2) impact of normalization on consensus scores,
 984 and (3) impact of NLL estimation strategy.

986 F.1 SELECTION FREQUENCY DISTRIBUTION

988 To understand how the consensus mechanism selects draft experts, we analyze the selection fre-
 989 quency of each model across benchmarks. Table 14 reports the proportion of instances in which
 990 each model is selected. All models participate with non-trivial frequencies (38.6%–84.7%), with
 991 no model dominating or being marginalized. This indicates that different drafts specialize in dif-
 992 ferent subsets of questions, and the consensus mechanism leverages complementary agreement and
 993 disagreement across experts rather than collapsing to a single always-selected model.

995 Table 14: Selection frequency of each draft model across benchmarks.

996 Model	997 InfographicVQA	998 ChartQAPro
999 Qwen2.5-VL-7B-Instruct	84.7%	77.7%
1000 GLM-4.1V-9B-Thinking	38.6%	69.3%
1001 MiMO-VL-7B-RL	54.8%	56.8%
1002 InternVL3-8B	73.4%	53.1%
1003 Ovis2.5-9B	48.5%	43.1%

1004 F.2 IMPACT OF NORMALIZATION ON CONSENSUS SCORES

1005 We further ablate the effect of normalization on consensus scores, which is motivated by the calibra-
 1006 tion gap across draft experts mentioned in Section 3.4. Different VLMs produce perplexity scores on
 1007 systematically different numerical scales due to training and tokenization differences. In our pool,
 1008 for example, Qwen2.5-VL and GLM-4.1V-Thinking tend to output larger-magnitude NLLs. With-
 1009 out normalization, such scale mismatch causes high-magnitude models to dominate the consensus
 1010 even when they do not genuinely agree more often, thereby reducing selection diversity.

1011 We evaluate normalization on two draft pools on InfographicVQA: (i) the main pool used in our
 1012 primary experiments, mixing reasoning and non-reasoning drafts, and (ii) an additional pool con-
 1013 sisting only of non-reasoning drafts, introduced in Appendix E. Tables 15a and 15c show that, on
 1014 the main pool, removing normalization collapses selection to a near-fixed subset: Qwen and GLM
 1015 are selected in almost all instances. This collapse hurts performance on ChartQAPro, demonstrating
 1016 that calibration artifacts can actively degrade consensus quality. Although InfographicVQA remains
 1017 similar without normalization, this results from an accidental strong pairing being repeatedly se-
 1018 lected rather than a principled aggregation.

1019 To verify that this trend is not pool-specific, we repeat the ablation on the additional non-reasoning
 1020 pool. Tables 15b and 15d show the same selection-collapse pattern without normalization, together
 1021 with a clear performance drop. Across both pools, normalization mitigates calibration bias, prevents
 1022 dominance by a few drafts, and yields more stable performance.

1024 F.3 IMPACT OF NLL ESTIMATION STRATEGY

1026

1027

Table 15: Normalization ablations on the main and additional draft pools.

1028

(a) Ablations on normalization on the main draft pool.

1029

Variant	InfographicVQA	ChartQAPro
SV w/o norm.	88.9	59.4
SV	88.4	64.0

1030

1031

1032

1033

1034

1035

(c) Selection frequency on the main pool without normalization.

1036

Model	InfographicVQA	ChartQAPro
Qwen2.5-VL-7B-Instruct	99.9%	100.0%
GLM-4.1V-9B-Thinking	77.1%	99.9%
MiMO-VL-7B-RL	57.0%	71.5%
InternVL3-8B	47.0%	21.4%
Ovis2.5-9B	19.1%	2.2%

1037

1038

1039

1040

1041

1042

1043

1044

1045

1046

1047

1048

(b) Ablations on normalization on the additional non-reasoning pool.

Variant	InfographicVQA
SV w/o norm.	84.6
SV	86.3

(d) Selection frequency on the additional non-reasoning pool.

Model	w/ norm.	w/o norm.
Qwen2.5-VL-7B-Instruct	87.3%	99.9%
Eagle2.5-8B	65.4%	98.0%
LLaVA-OneVision-1.5-8B	28.6%	79.3%
InternVL3-8B	74.5%	16.7%
Ovis2.5-9B	44.2%	6.11%

We examine whether computing NLL only on final answers introduces off-policy bias, since draft experts’ answers are generated together with reasoning trajectories. Table 16 compares expert selection using answer-only NLL (SV) versus full-trajectory NLL. The two variants achieve very similar performance, suggesting that any off-policy bias from answer-only scoring is negligible for this task. Moreover, answer-only scoring is more computationally efficient, as it avoids computing NLL over long reasoning traces with many extra tokens; answer-only NLL also provides a cleaner signal by avoiding noise from diverse reasoning styles across models. We therefore use answer-only NLL in the main experiments.

1049

1050

Table 16: Ablation on NLL estimation strategy.

1051

1052

1053

1054

1055

1056

G COMPARISON TO LLaVA-CRITIC (LMM-AS-A-JUDGE BASELINE)

1057

1058

We compare SV to a learned LMM-as-a-Judge baseline, LLaVA-Critic (Xiong et al., 2025). LLaVA-Critic is trained as a generalist multimodal evaluator that jointly leverages visual evidence and textual reasoning to score or rank multiple candidates.

1061

1062

1063

1064

1065

1066

1067

1068

1069

1070

1071

1072

1073

1074

1075

1076

1077

1078

1079

Experimental setup. We follow the official LLaVA-Critic evaluation template and consider two judging modes: (i) pointwise scoring, where the judge assigns a scalar score to each candidate and selects the highest-scored one; (ii) pairwise ranking, where candidates are compared (i.e., first two candidates are compared, and the winner is then compared against the third in our scenario). To ensure a comprehensive comparison, we evaluate LLaVA-Critic under two settings: (1) judging the same three consensus experts selected by SV (directly replacing the verdict); (2) judging five candidate models. In all cases, the judge outputs a single best candidate.

For SV, we conduct experiments with two verdict models: GPT-4o and LLaVA-OneVision-7B (Li et al., 2024). GPT-4o serves as a strong proprietary verdict model, matching our main experiments, while LLaVA-OneVision-7B shares the same backbone as LLaVA-Critic, enabling a fairer comparison in the open-source regime.

Results. Table 17 shows that when judging the same three draft experts, SV consistently outperforms LLaVA-Critic-7B across all three benchmarks under both verdict choices. With GPT-4o as the verdict, SV improves over LLaVA-Critic-7B by 4.9–11.9%. With LLaVA-OneVision-7B as the verdict, SV still yields gains of 0.5–6.6%, which demonstrates that the advantage stems from SV’s design rather than from verdict model superiority alone.

This gap is attributed to the different aggregation principles: LLaVA-Critic performs *selection*-based judging and can only pick one trajectory, while SV performs *synthesis*-based verification, cross-checking and integrating complementary factual cues across trajectories. In practice, the critic is

1080
1081
1082
1083
1084
1085
1086
1087
1088
1089
1090
1091
1092
1093
1094
1095
1096
1097
1098
1099
1100
1101
1102
1103
1104
1105
1106
1107
1108
1109
1110
1111
1112
1113
1114
1115
1116
1117
1118
1119
1120
1121
1122
1123
1124
1125
1126
1127
1128
1129
1130
1131
1132
1133
Table 17: Performance of SV and LLaVA-Critic-7B.

Method	InfographicVQA	ChartMuseum	ChartQAPro
LLaVA-Critic-7B (pointwise)	83.5	40.1	52.4
LLaVA-Critic-7B (pairwise)	81.4	38.9	52.1
SV w/ GPT-4o verdict	88.4	49.3	64.0
SV w/ LLaVA-OneVision-7B verdict	<u>84.0</u>	<u>44.1</u>	<u>59.0</u>

Table 18: Average judge/verdict tokens per sample.

Method	InfographicVQA	ChartMuseum	ChartQAPro
LLaVA-Critic-7B (pointwise)	1053.3	3723.7	1290.7
LLaVA-Critic-7B (pairwise)	1342.9	4689.4	1759.1
SV w/ GPT-4o verdict	701.7	3122.3	1441.7
SV w/ LLaVA-OneVision-7B verdict	702.4	3123.0	1442.4

Table 19: Performance of SV and LLaVA-Critic-7B judging five candidate models (1k samples).

Method	InfographicVQA	ChartMuseum	ChartQAPro
LLaVA-Critic-7B (pointwise)	82.3	34.6	56.5
SV w/ GPT-4o verdict	88.3	49.3	63.4
SV w/ LLaVA-OneVision-7B verdict	<u>83.6</u>	<u>44.1</u>	<u>57.8</u>

Table 20: Performance of SV and LLaVA-Critic-72B judging three consensus experts (1k samples).

Method	InfographicVQA	ChartMuseum	ChartQAPro
LLaVA-Critic-72B (pointwise)	82.6	40.4	53.5
LLaVA-Critic-72B (pairwise)	83.1	43.0	55.8
SV w/ GPT-4o verdict	88.3	49.3	63.4
SV w/ LLaVA-OneVision-7B verdict	<u>83.6</u>	<u>44.1</u>	<u>57.8</u>

also more sensitive to surface form (e.g., verbosity, repetitiveness, or stylistic fluency), whereas SV is guided by consensus evidence and is therefore more robust to such artifacts.

Table 18 further reports the total judge/verdict tokens. Under comparable prefill-based budgets, SV achieves higher performance with similar or lower token usage on InfographicVQA and ChartMuseum, and still attains a much better cost–performance trade-off on ChartQAPro.

When increasing the candidate pool to five models (Table 19), LLaVA-Critic-7B remains clearly below SV, indicating that simply adding more candidates to a selection-based judge does not close the gap. Finally, even a much larger judge (LLaVA-Critic-72B, Table 20) is still notably weaker than SV, even including the variant with the smaller LLaVA-OneVision-7B verdict. This confirms that SV is more effective than selection-based judging for information-intensive visual reasoning.

H ABLATION STUDIES ON VERDICT INPUT CONFIGURATION

H.1 IMPACT OF VISUAL INPUT TO VERDICT

We examine whether visual input is necessary for the verdict or if reasoning paths alone suffice. Table 21 presents results where the verdict receives only textual reasoning paths without image input. The results show that SV without visual input achieves modest gains over the reasoning baseline on InfographicVQA, and even underperforms on ChartMuseum and ChartQAPro. In contrast, incorporating visual input for verdict yields substantial improvements across all benchmarks. These results demonstrate that visual grounding is essential for the verdict to cross-check the factual accuracy of extracted information and distinguish correct from incorrect interpretations of the image.

H.2 IMPACT OF STRUCTURED IMAGE INPUT TO VERDICT

In our experimental setup in Section 4.1, we preprocess each image via PP-StructureV3, a document parsing model that generates Markdown representations capturing layout, textual blocks, and visual

1134
1135
1136 Table 21: Ablations on visual input to the verdict GPT-4o.
1137
1138
1139
1140

Method	InfographicVQA ANLS	ChartMuseum Acc	ChartQAPro Acc
Reasoning baseline	84.8	48.0	57.3
GPT-4o Verdict w/o input	85.9	47.1	53.2
GPT-4o Verdict w/ input (SV)	88.4	49.3	64.0

1141
1142 Table 22: Ablations on additional structured image input to the verdict GPT-4o.
1143
1144

Method	InfographicVQA ANLS	ChartMuseum Acc	ChartQAPro Acc
Reasoning baseline	84.8	48.0	57.3
GPT-4o Verdict w/o input	88.3	49.5	59.4
GPT-4o Verdict w/ input (SV)	88.4	49.3	64.0

1149 metadata (Cui et al., 2025). This structured representation is then rendered as an image and provided
1150 as an additional image input for the verdict. This allows the verdict to access both the raw visual
1151 content and a layout-aware text representation simultaneously. To verify whether this input is critical
1152 or merely auxiliary, we conduct an ablation study (Table 22).

1153 The results show that SV achieves substantial gains over the reasoning baseline even without struc-
1154 tured input. With the structured input, performance is generally slightly improved, though the gain
1155 is negligible or even marginally lower in some cases. This pattern suggests that structured OCR-
1156 derived signals are not essential for SV’s core performance, but may assist the verdict to distinguish
1157 among competing reasoning paths.

1159 I QUANTITATIVE ANALYSIS OF DRAFT COMPLEMENTARITY

1160 To characterize the complementarity of draft experts, we focus on minority-correct recovery cases
1161 on InfographicVQA where only one of the three selected experts is correct and SV subsequently
1162 recovers the correct answer. These cases are most diagnostic for understanding how specific models
1163 provide unique, correct information and how others behave to help the verdict distinguish cues.

1164 We randomly sample 50 minority-correct recovery instances and manually categorize their dominant
1165 reasoning bottlenecks into five types, summarized in Table 23. Extraction-related failures account
1166 for half of the cases, followed by color matching and global scan.

1167
1168 Table 23: Distribution of dominant reasoning bottlenecks over 50 minority-correct recovery cases
1169 on InfographicVQA.

Reasoning bottleneck	Description	Frequency (%)
Extraction	Locating and reading fine-grained text/numbers	50
Color matching	Matching colors in legends/charts to labels	18
Global scan	Aggregating evidence across the full image	16
Localization	Finding query-relevant regions	10
Numerical comparison	Comparing numerical values	4

1170 Table 24 reports per-model success rates within each bottleneck category over the 50 minority-
1171 correct instances. We observe a clear division of labor across experts: GLM-4.1V-Thinking and
1172 MiMO-VL-RL are most reliable for fine-grained extraction (58% and 70% success, respectively),
1173 with MiMO additionally strong on global-scan cases (75%). This advantage is consistent with their
1174 reasoning-oriented behavior: their step-by-step trajectories enable iterative verification of extracted
1175 values and cross-checking across multiple regions. Ovis2.5 and GLM-4.1V-Thinking perform best
1176 on color matching (57% and 60%), while Qwen2.5-VL dominates localization (80%) and numer-
1177 ical comparison (100%). We find that other experts often fail in these categories due to keyword-
1178 comprehension errors, whereas Qwen2.5-VL’s correct grounding makes its answer salient for the
1179 verdict to identify even when other models provide detailed but misdirected reasoning. Overall,

1188 no single expert dominates all reasoning types, confirming that SV benefits from specialized and
 1189 complementary strengths rather than redundant voting.
 1190

1191
 1192 Table 24: Per-model success rates (%) on minority-correct recovery cases, broken down by reasoning
 1193 bottleneck.

Reasoning type	Qwen2.5-VL-Instruct	GLM-4.1V-Thinking	MiMO-VL-RL	Ovis2.5	InternVL3
Extraction	15	58	70	38	15
Color matching	0	60	33	57	25
Localization	80	0	0	33	0
Global scan	0	33	75	20	0
Numerical comparison	100	0	0	0	0

1200
 1201 Finally, we summarize the most frequent expert combinations all 243 minority-correct recovery
 1202 cases on InfographicVQA, as shown in Table 25. Two typical complementarity patterns emerge.
 1203 First, balanced visual-skill combinations (e.g., Qwen–Ovis–InternVL) appear in cases requiring
 1204 diverse perceptual cues. Second, extraction-focused pairings (e.g., Qwen–MiMO–InternVL and
 1205 Qwen–GLM–Ovis) arise in extraction-intensive problems, where reasoning drafts provide accurate
 1206 fine-grained values and non-reasoning drafts contribute robust localization for cross-verification.
 1207 Overall, this analysis supports our claim that SV does not simply average similar models: it ex-
 1208 ploits complementary reasoning strengths across draft experts, and the minority-correct recoveries
 1209 we observe are closely associated with diverse and specialized reasoning trajectories across models.
 1210

1210 Table 25: Most frequent expert combinations among all minority-correct cases on InfographicVQA.

Rank	Model combination	Frequency (%)
1	Qwen + Ovis + InternVL	33.3
2	Qwen + MiMO + InternVL	14.0
3	Qwen + GLM + Ovis	11.1

J FAILURE MODE ANALYSIS OF SV

1220 We analyze cases where the majority of selected draft experts are correct but SV produces an incor-
 1221 rect answer on InfographicVQA with GPT-4o as verdict. These instances isolate failures when the
 1222 consensus mechanism or verdict synthesis fails despite having correct information available. Under
 1223 exact-match scoring, such cases account for 3.98% of majority-correct examples; after normalizing
 1224 answer formats (e.g., “Feb 11” vs. “February 11”), the true failure rate is 1.34% (34 cases).

1225 **Failure modes.** Two dominant patterns emerge. (i) Fine-grained extraction errors (52.9%) arise
 1226 from tiny numbers or small text on very tall infographics. Although draft experts often extract the
 1227 correct cue, GPT-4o may fail to verify it because its tile-based high-resolution pipeline downsamples
 1228 long inputs, losing subtle details. (ii) Color matching errors (35.3%) require aligning colored legends
 1229 or regions with labels. This reflects a shared VLM capability gap: when both drafts and verdict
 1230 struggle with color discrimination, drafts provide uncertain reasoning (sometimes explicit guesses),
 1231 and GPT-4o exhibits verbosity bias in 58.3% of such cases (i.e., it follows the draft with the longest
 1232 trajectory despite majority consensus pointing elsewhere).

1233 Overall, SV inherits current VLM weaknesses in precise color reasoning and fine-grained percep-
 1234 tion, and when visual evidence is ambiguous the verdict may over-weight fluent yet incorrect drafts.
 1235

1236 Table 26: Breakdown of SV failure modes on InfographicVQA.

Failure mode	Proportion
Fine-grained extraction	52.9%
Color matching	35.3%
Other	11.8%

1242 K FAILURE MODE ANALYSIS OF TOOL-DRIVEN PIPELINE

1244 As mentioned in Section 2, tool-driven methods represent a line of work that augments vision-
 1245 language reasoning with explicit zoom-in operations. The representative pipeline DeepEyes is de-
 1246 signed to iteratively ground into image regions, and integrate them into the ongoing reasoning trajec-
 1247 tory under an RL framework. This mechanism has proven effective on high-resolution benchmarks,
 1248 where localized inspection of fine details is crucial.

1249 However, DeepEyes is not specifically trained on our benchmarks, which require reasoning over
 1250 information-intensive images with densely interleaved textual and visual elements. Its performance
 1251 on InfographicVQA reveals the current limitations of such tool-based pipelines in this domain. We
 1252 categorize the observed deficiencies into three core challenges:

1253 (i) Tendency toward literal grounding. DeepEyes is proficient at small-scale grounding but often
 1254 focuses on literal text spans or legends rather than reasoning-critical regions. For example, when a
 1255 question requires aligning numerical values with a chart axis, the model frequently grounds directly
 1256 onto the answer text or nearby labels instead of the relevant data regions. This shortcut strategy
 1257 works for simple queries but fails on complex reasoning on information-intensive images that require
 1258 global comparison.

1259 (ii) Inefficient tool usage. Although DeepEyes is trained to iteratively apply zoom-in tools, we
 1260 observe that it invokes only one zoom step in more than half of the test cases. Among the double-
 1261 zoom cases, 92.8% duplicate the same bounding box, which serves only for verification rather than
 1262 exploration. In some instances, the model zooms into empty areas or irrelevant regions.

1263 (iii) Lack of robustness on long and dense images. Information-intensive images often contain multi-
 1264 panel figures and dense annotations. DeepEyes cannot maintain a trajectory across multiple zoom
 1265 steps, making it difficult to integrate dispersed evidence. As a result, tasks requiring cross-region
 1266 synthesis, such as counting, sorting, or comparing across multiple subplots, remain challenging.

1267 Overall, this analysis indicates that while tool-driven pipelines are promising for high-resolution
 1268 inspection tasks, they face notable difficulties applying to information-intensive images without
 1269 domain-specific supervision. In contrast, SV achieves strong performance without additional train-
 1270 ing, offering a simple and effective alternative for reasoning over complex multimodal inputs.

1273 L QUALITATIVE EXAMPLE

1275 Figure 9 illustrates a case where all three draft experts produced incorrect reasoning paths, yet
 1276 the verdict successfully corrected the answer. Specifically, the draft experts faced different types
 1277 of failures: some mis-extracted information from the image, others extracted the key information
 1278 correctly but failed to sort the values properly, and thus all generated wrong answers. Interestingly,
 1279 the verdict itself, when asked directly, also tends to answer “Australia” incorrectly. However, when
 1280 analyzing the noisy and conflicting reasoning paths together, the verdict was able to recover the
 1281 correct answer (Portugal).

1282 This example complements the main results section: while Figure 3 illustrates recovery from
 1283 minority-correct experts, here we present a zero-correct case to show that SV can still synthesize
 1284 the correct solution even when all drafts and the verdict individually fail.

1286 M PROMPT TEMPLATES

1288 M.1 CHAIN-OF-THOUGHT PROMPTS

1290 As described in Section 4.1, we employ a Chain-of-Thought prompt for each consensus expert to
 1291 generate reasoning paths and apply it identically when evaluating baselines. For InfographicVQA
 1292 and HR-Bench 4K, we use the same CoT prompt. For ChartMuseum (Tang et al., 2025), we adopt
 1293 its official reasoning prompt, and adapt that prompt strategy to ChartQAPro, given their simila-
 1294 rity in task complexity. Since ChartQAPro requires different prompt templates tailored to question
 1295 types (Masry et al., 2025), we first follow its official template per question type, then concatenate it
 1296 with our reasoning prompt.

1296 The reasoning prompts for these datasets are shown in Figure 10.
1297

1298 **M.2 PROMPTS FOR VERDICT**
1299

1300 The user prompts used in the verdict stage are identical across datasets except for the final instruction
1301 sentence, which is customized (see Figure 12). For GPT-4o as verdict, the system prompt is shown in
1302 Figure 11. For Qwen-2.5-VL-72B-Instruct as verdict, we prepend its system prompt at the beginning
1303 of the user prompt.

1304

1305 **N THE USE OF LARGE LANGUAGE MODELS (LLMs)**
1306

1307 In this work, we used LLMs solely for auxiliary tasks such as language polishing, prompt refining,
1308 and proofreading. Importantly, these interventions did not contribute any main scientific insight,
1309 experimental design, or methodological advance. All core ideas, theoretical developments, experi-
1310 ments, analyses, and claims in this paper are the work of the authors. Accordingly, authors assume
1311 full responsibility for all content, consistent with ICLR policy that LLMs are not eligible for author-
1312 ship.

1313

1314

1315

1316

1317

1318

1319

1320

1321

1322

1323

1324

1325

1326

1327

1328

1329

1330

1331

1332

1333

1334

1335

1336

1337

1338

1339

1340

1341

1342

1343

1344

1345

1346

1347

1348

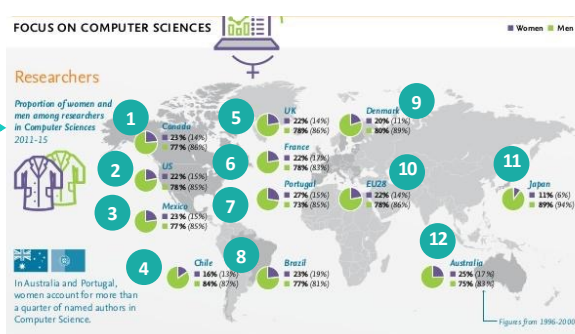
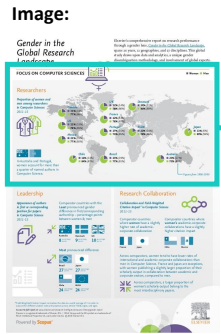
1349

1350
1351
1352
1353
1354
1355
1356

1357 **Question:** In which country the percentage of female
1358 researcher was the highest in the duration of 2011-15?

1359 **Ground-truth: Portugal**

1360
1361
1362
1363
1364
1365
1366
1367
1368
1369



1370
1371
1372
1373
1374
1375
1376
1377
1378
1379
1380
1381
1382
1383
1384
1385
1386
1387
1388
1389
1390
1391
1392
1393
1394



To determine the country with the highest percentage of female researchers in the duration of 2011-15, let's analyze the data provided in the image:

1. The image shows a pie chart for each country, indicating the proportion of women and men among researchers in Computer Sciences for the years 2011-15.
2. We need to compare the percentages of women researchers for each country listed.

Here are the percentages for each country:

Canada: 23% (women), US: 22% (women), Mexico: 23% (women), Chile: 16% (women), Brazil: 23% (women), EU28: 22% (women), Australia: 25% (women), Denmark: 20% (women), France: 22% (women), Portugal: 27% (women), Japan: 11% (women)

From the above percentages, the highest percentage of women researchers is in **Australia** at 25%.



To answer the question, we need to look at the section titled "Researchers" which shows the proportion of women and men among researchers in Computer Sciences from 2011-15. Each country is represented by a circle with two segments, one for women and one for men, with the percentage values indicated. We need to identify the country with the largest segment for women:

Canada: 33% women, UK: 24% women, France: 22% women, US: 22% women, Mexico: 18% women, Peru: 17% women, Chile: 16% women, Brazil: 23% women, Australia: 25% women, Japan: 11% women, Denmark: 11% women, Portugal: 26% women, ELIZABET: 22% women

From the list, we can see that **Canada** has the highest percentage of female researchers at 33%.



To determine the country with the highest percentage of female researchers (2011 - 15), we examine the "Researchers" section, which lists women's percentages (green) for each country. Checking each country's data: Canada: 23%, Denmark: 20%, France: 78%, US: 22%, Portugal: 27% (women), Mexico: 23%, Australia: 29%, Brazil: 23%, UK: 22%, EU28: 22%, Chile: 16%

Among these, **France** has the highest percentage of female researchers at 78%.



1395 Figure 9: A qualitative zero-correct case corrected by verdict. All three draft experts fail due to
1396 errors in extracting or sorting visual information, yet the verdict synthesizes their noisy reasoning
1397 paths to recover the correct answer (i.e., Portugal).
1398

1399
1400
1401
1402
1403

1404
1405
1406
1407
1408
1409

1410 InfographicVQA / HR-Bench 4K

1411
1412
1413
1414
1415

Question: {QUESTION} Please think step-by-step about the image to answer the question using a single word or phrase enclosed within \boxed{{}}.

1416
1417
1418
1419
1420
1421
1422
1423
1424
1425
1426
1427
1428
1429
1430
1431
1432
1433
1434
1435
1436
1437
1438
1439
1440
1441
1442

ChartMuseum

Please answer the question using the chart image.

Question: {QUESTION}

Please first generate your reasoning process and then provide the user with the answer. Use the following format:

```
<think>
... your thinking process here ...
</think>
<answer>
... your final answer (entity(s) or number) ...
</answer>
```

ChartQAPro

{PROMPT for a specific question type}

Please first generate your reasoning process and then provide the user with the answer. Use the following format:

```
<think>
... your thinking process here ...
</think>
<answer>
... your final answer (entity(s) or number) ...
</answer>
```

1443
1444
1445

Figure 10: Prompt templates for reasoning.

1446
1447
1448
1449
1450
1451
1452
1453
1454
1455
1456
1457

All benchmarks

You are a vision-and-language judge. Follow the instructions strictly.
.

Figure 11: System prompt template for verdict.

```

1458 InfographicVQA / ChartMuseum
1459
1460 Question:
1461 {QUESTION}
1462 --- Model 1 ---
1463 Reasoning:
1464 {Reasoning path 1}
1465 Proposed Answer: {Answer 1}
1466 --- Model 2 ---
1467 Reasoning:
1468 {Reasoning path 2}
1469 Proposed Answer: {Answer 2}
1470 --- Model 3 ---
1471 Reasoning:
1472 {Reasoning path 3}
1473 Proposed Answer: {Answer 3}
1474 Given the raw image, the layout-annotated image, the question, and
1475 the reasoning from three models, please give the final answer using a
1476 single word or phrase enclosed within \boxed{}.
1477
1478 ChartQAPro
1479
1480 Question:
1481 {QUESTION}
1482 --- Model 1 ---
1483 Reasoning:
1484 {Reasoning path 1}
1485 Proposed Answer: {Answer 1}
1486 --- Model 2 ---
1487 Reasoning:
1488 {Reasoning path 2}
1489 Proposed Answer: {Answer 2}
1490 --- Model 3 ---
1491 Reasoning:
1492 {Reasoning path 3}
1493 Proposed Answer: {Answer 3}
1494 Given the raw image, the layout-annotated image, the question, and
1495 the reasoning from three models, please directly give the final
1496 answer enclosed within \boxed{}.
1497
1498 HR-Bench 4K
1499
1500 Question:
1501 {QUESTION}
1502 --- Model 1 ---
1503 Reasoning:
1504 {Reasoning path 1}
1505 Proposed Answer: {Answer 1}
1506 --- Model 2 ---
1507 Reasoning:
1508 {Reasoning path 2}
1509 Proposed Answer: {Answer 2}
1510 --- Model 3 ---
1511 Reasoning:
1512 {Reasoning path 3}
1513 Proposed Answer: {Answer 3}
1514 Given the image, the question, and the reasoning from three models,
1515 please directly give the final answer with the option's letter
1516 enclosed within \boxed{}.
1517
1518

```

Figure 12: User prompt templates for verdict.